The Florida State University
DigiNole Commons

Honors Theses | Division of Undergraduate Studies

4-1-2012

Using Boundary Element-Based Near-field Acoustic Holography to Predict the Source Pressures and Sound Field of an Acoustic Guitar

Benjamin Goldsberry
Florida State University, bmg08c@my.fsu.edu

Recommended Citation
Goldsberry, Benjamin, "Using Boundary Element-Based Near-field Acoustic Holography to Predict the Source Pressures and Sound Field of an Acoustic Guitar" (2012). *Honors Theses*. Paper 88.
http://diginole.lib.fsu.edu/uhm/88

This Open Access Honors Thesis is brought to you for free and open access by the Division of Undergraduate Studies at DigiNole Commons. It has been accepted for inclusion in Honors Theses by an authorized administrator of DigiNole Commons. For more information, please contact lib-ir@fsu.edu.

Abstract:
(Near-field Acoustic Holography, Audio Production, Guitar)
In recording studios, the placement of microphones to record an acoustic guitar is very much subjected to trial and error and audio engineer preference. In order to make more informed microphone placement decisions, Near-field Acoustic Holography is used to study the sound pressures of the guitar. This technique involves solving the integral formulation of the Helmholtz equation over the surface of the guitar. By measuring the acoustic pressures surrounding the guitar, an inverse problem can be solved to derive the pressures on the surface of the guitar. Then, the surface pressures are used to study the pressure propagations in the far-field. Using the superposition of waves principle, chords played on the guitar can be studied by summing the pressure waves of the three notes that make a chord. Studying the wave fields are then used to either validate current microphone techniques, or require new microphone placements and patterns.

THE FLORIDA STATE UNIVERSITY

COLLEGE OF ARTS AND SCIENCES

USING BOUNDARY ELEMENT-BASED NEAR-FIELD ACOUSTIC HOLOGRAPHY TO PREDICT THE SOURCE PRESSURES AND SOUND FIELD OF AN ACOUSTIC GUITAR

By

Benjamin Goldsberry

A Thesis submitted to the
Department of Mathematics
in partial fulfillment of the requirements for graduation with
Honors in the Major

Degree Awarded:
Spring, 2012

The members of the Defense Committee approve the thesis of Benjamin Goldsberry defended on April 9, 2012.

_____

Dr. Mark Sussman
Thesis Director

_____

Dr. Brian Gaber
Outside Committee Member

_____

Dr. Nick Cogan
Committee Member

Table of Contents

Introduction: Motivation for Study

The guitar is arguably one of the most diverse instruments in the musical family. First of all, most instruments are only seen in a few musical genres. For example, the cello is usually only seen as a classical music instrument, while the saxophone is seen primarily as a jazz instrument. The guitar is the only instrument, with the exception of the keyboard, to be very prominent in a diverse range of musical styles, from classical to heavy metal. Because of the guitar's popularity in these styles, it is the only instrument, again with the exception of the keyboard, to have a variety of shapes and sounds. The guitar family is subdivided into three branches: nylon-stringed guitars, steel-stringed guitars, and electric guitars. Within these three branches are even more subdivisions, with each guitar model creating a unique perspective on both the aesthetic portions and the sonic qualities of the guitar. The broad existence of guitar shapes and sounds creates an opportunity for a researcher to study how all of these variations can change the sound.

Another unique feature of the guitar that separates it from the other instruments is its ability to play both melodic (one note at a time) and polyphonic (multiple notes at one time) lines. This is in direct contrast to a purely monophonic instrument, such as the flute, which plays only one note at a time. In more contemporary styles, such as rock and country, the guitar plays a more accompanying role by providing a harmonic structure, in the form of chords, to a piece of music.

Because the guitar has many characteristics, it is important to limit research to one less-known characteristic. As a guitar player and audio engineer, I have decided to focus on the sound radiation of the acoustic guitar and how this affects microphone placement techniques. In the music and audio engineering world, the advice given to new engineers on how to mic a guitar is to “use your ears.” Miking an acoustic guitar is then subjected to what kind of guitar it is, how the person is playing it, and what the audio engineer running the session thinks is a good guitar sound. With many variables to think about, new audio engineers quickly become overwhelmed with the infinite amount of ways to mic a

guitar. Like learning how to play an instrument, it is only through experience of miking guitars and developing a good ear that you then become good at it.

Therefore, I want to use mathematical techniques to help aid decisions on microphone placements around a guitar. Since guitarists usually play chords in the popular genres of music, the aim of my research is to investigate what a pressure field surrounding a guitar would be if a chord was played. Using the pressure field data, one can then determine whether current microphone placement techniques are validated, or if new microphone techniques will provide a more optimal sound. The outcome can then be used to help aid the engineer on where to place microphones. The subjectivity of microphone placements for a guitar is then lessened with mathematical certainty. In addition, it is very important for the implementation to be cost-effective and time efficient, so that studios and audio engineers are more willing to implement my research into their recording sessions. With all of these ideas in mind, I decided to use the mathematical technique Near-field Acoustic Holography (NAH) to find the acoustic pressures around the guitar. NAH is primarily used to study complex sound sources, such as jets and automobiles, and for reasons to be discussed, provides an excellent way to measure the pressures of an acoustic guitar. In the following chapters, I will first describe what is known about the guitar and recording techniques, then what NAH is and how it can be implemented. I will then implement NAH for the guitar and show the conclusions, ending with ideas for more optimal microphone placements and future research ideas.

Chapter 1: Prior Studies of the Guitar

1.1 Empirical and Analytical Studies

Many physical properties of the guitar have been extensively studied.[1,2] These studies range from physically observing how guitars work to complete mathematical interpretations. Most of these studies have two purposes. The first is to aid in guitar construction. This is particularly important since many guitars are being mass produced in factories. In order for a guitar to be consistent with another of the same brand, constant building habits must be in order, and therefore an understanding of how the guitar physically behaves is required. The second purpose is to mathematically model a guitar so that the sound can be artificially reproduced. Since the development of MIDI in the 1980's, artificially reproduced instruments have become popular as an inexpensive substitute to live musician performances on a recording.[3] Many developments are materializing in the modeling field to produce accurate sounds so that the listener cannot tell the difference between a real and artificially reproduced instrument.

In regards to engineering the guitar, many of the physical properties of the guitar are discussed in the book Engineering the Guitar by Richard French. When studying the physics of the guitar, one must first consider the strings and how the strings interact with the guitar body. This is a fundamental property shared by all guitars. “All guitars, no matter the type, have components in common and are subject to the same types of loads.”[4] The strings exert a tremendous amount of tension, and French goes into mathematical detail on how string forces and tension affect the guitar. This is a very important part in guitar construction and must not be overlooked because the design must be able to withstand and hold the tension of the strings.

---

1 Richard Mark French, *Engineering the Guitar: Theory and Practice* (New York: Springer Science, 2009).
2 Daniel Russell, “Acoustics and Vibrations of Guitars,” Penn State Acoustics, http://www.acs.psu.edu/drussell/guitars.html (accessed March 5, 2012).
3 David Miles Huber and Robert E. Runstein, *Modern Recording Techniques 7th Edition* (Oxford: Focal Press, 2010), 309.
4 French, *Engineering the Guitar: Theory and Practice*, 43.

> "The strings must be brought to the correct tension for the instrument to be in tune, so the neck and body must resist the resulting compressive load. In addition, there are dynamic loads when the instrument is played. Finally, there are forces generated by temperature and humidity changes. While these might not be the most obvious sources of loading, they are a very common source of structural failure. It makes sense, then, to explore the structure of guitars and how they are designed to be strong enough to withstand both playing and environmental loads while being light enough to radiate sound."[5]

While optimizing the tonal qualities of a guitar is very important, the guitar must also be playable. In regards to designing a guitar neck, "The neck also has to have a profile that makes it comfortable to play; it cannot be so wide or thick that it is difficult to grasp, nor so narrow or shallow that it is difficult to play."[6] Sometimes, most luthiers must go through a give and take between optimization of sound and playability.

The part of the guitar that aids the body in holding the string tension is the bracing pattern. "The purpose of bracing is to increase the stiffness of the top plate enough for it to withstand string tension without making the plate so stiff or heavy that it can't respond to the string motion."[7] Many bracing patterns exist for the guitar, and it has a substantial impact on the tonal qualities. While most of the bracing designs evolved empirically from trial and error, some guitars are built analytically by studying the underlying physics of how guitar bodies vibrate, and are designed so that the body will respond in a particular way at different frequencies. An example of an analytical bracing pattern is the Kasha-Schneider pattern. The bracing pattern is asymmetric, and is intended to match the bridge to the mechanical impedance of the soundboard.[8] Another important aspect of the guitar body is the construction material. "Traditionally, all guitars have been made out of wood. Unlike most violin makers, guitar makers have been quite willing to make instruments from just about any wood available."[9] The most popular woods for the top plate are spruce and cedar, while the popular woods for

5 Ibid., 43.
6 Ibid., 43.
7 Ibid., 64.
8 Ibid., 65.
9 Ibid., 93.

the back plate and sides are rosewood, maple, and mahogany.[10]

The next important study of the physics of guitars is how it radiates sound. This has been mostly studied by observing the modes, or the resonant frequencies, of the guitar. These modes vary in shape and form because there are so many variations on guitar designs. “Generalizing mode shapes is difficult since there is so much variation in the design of acoustic guitars.”[11] Dr. Daniel Russell has done many experimental observations on the modes of guitars. Russell has investigated the modes of traditional shaped electric guitars, non-traditional shaped electric guitars, and acoustic guitars. To study the modes, an impact hammer was used to drive the guitar to a resonate state, and an accelerometer was used to gather the data. The data shows that at low frequencies, a major portion of the guitar vibrates, and the front and back plates vibrate out of phase with each other. In the middle frequency modes (223Hz-315Hz), the front and back plates vibrate in phase with each other, and there are more surface nodal lines present than the lower frequencies. At the high frequency modes (>385Hz), more surface nodal lines are present, with parts of the guitar vibrating out of phase with other parts. The out of phase vibrational patterns make the guitar an ineffective radiator of sound at high frequencies.[12]

In addition to physically studying the guitar through observation, many attempts on mathematically modeling the guitar have been made.[13,14] Mathematically describing a guitar provides consistency in guitar building, a means to artificially create guitar sounds, and it assists in designing more optimized guitar models. However, like many complex systems, mathematically modeling the guitar is very challenging because of the complexity of coupling and solving the many relevant equations. “Historically, stringed instruments have been designed empirically, and progress on describing them using mathematical models was slow until the mid 20th century. Stringed musical

10 Ibid., 93.
11 Ibid., 118.
12 Russell, “Acoustics and Vibrations of Guitars.”
13 Gregoire Derveaux et al., “Numerical Simulation of a Guitar,” *Computers and Structures* 83 (2005).
14 Giuseppe Cuzzucoli et al., “A Physical Model of the Classical Guitar, Including the Player's Touch,” *Computer Music Journal* 83, no. 2 (1999).

instruments pose a surprisingly difficult challenge to the would-be analyst."[15] The two big papers that have dealt with modeling the guitar are "Numerical Simulation of a Guitar" by Gregoire Derveaux, and "A Physical Model of the Classical Guitar, Including the Player's Touch" by Giuseppe Cuzzucoli.

In "Numerical Simulation of a Guitar," Derveaux studies the guitar by solving a mathematical model numerically. Derveaux's approach does not directly integrate measured data into his method. Derveaux makes many assumptions: the amplitudes of vibration are small, which justify a linear model; the body has no thickness and the neck is neglected; the coupling between the string and the air is neglected; only the soundboard vibrates; only the transverse polarization of the string is considered, the in-plane displacement of the string (parallel to the soundboard) is neglected; and the string is excited with an idealized pluck. Therefore, the unknowns are the vertical displacement of the string, the vertical displacement of the soundboard, the acoustic pressure, and the acoustic velocity field. To solve for these unknown variables, equations for the string, soundboard, and the air are introduced and coupled so that the string equation results are the input for the soundboard equations, and so on. Derveaux then sets up the algorithm. First the system is at rest, and the string is under normal tension. Then, Derveaux uses the 1-D wave equation with a force exerted on the right-hand side of the string to describe how the string vibrates. The vertical force of the string is then used as input into the equations describing the flexural displacement of the soundboard. Acoustic radiation equations can then be used to translate the vibration of the plate to acoustic pressures in the air. Because the guitar is not a simple domain and the equations are not easy to solve, finite element methods are used. Also, since this problem is not time-periodic, the time variable is also discretized. When the algorithm was implemented, the numerical model agreed with experimental analysis on the modes. According to Derveaux, "Up to our knowledge, this is the first modeling of the instrument which involves the whole vibroacoustical behavior from the initial pluck to the 3D acoustic model."[16] An interesting note about

15 French, *Engineering the Guitar,* 131.
16 Derveaux, "Numerical Simulation of a Guitar," 124.

this model is that, since it includes the time variable, it also shows how the guitar body changes over time.

In the paper “A Physical Model of the Classical Guitar, including the Player's Touch,” Cuzzucoli had two goals. The first was to implement how the guitarist plucks the string. This idea is very important because the performer's approach to plucking the string substantially affects the sound quality of the instrument. Many musical pieces require that the guitarist pluck the strings in different ways so that tonal variations will “liven” the piece. In addition, tonal optimization can be achieved by plucking the guitar with the right combination of flesh and nail at a particular angle of attack, and with the right attack and release times.

This article was published in the Computer Music Journal, so Cuzzucoli's second goal in his paper was to develop a model with the intention to artificially reproduce a guitar sound on a computer. Many musicians have differing criticisms on artificially reproduced sounds. However, most musicians agree that reproduced instruments sound close to a real instrument, but qualities and features of the sound give away that it is indeed artificial. Most of this comes from the lack or un-incorporation of how the performer affects the instrument. By taking the player's touch into account, a more realistic guitar model can be achieved. Cuzzucoli uses the same algorithm and equations as Derveaux, except Cuzzucoli takes into account computer reproduction methods of sound, such as sampling. In addition, Cuzzucoli focuses more on the initial pluck interaction, since that is where the player's touch is present.

Cuzzucoli takes into account five parameters that affect how the string is plucked: the position of the plucking point along the string; the manner in which the string is excited; the manner in which the string is released; the interaction between the flesh or the nail and the vibrating string before the attack; and the initial displacement of the string resulting from the plucking force. “A realistic reproduction of the guitar sound can only result from a physical model that describes the player-

instrument interaction by taking into account the resources that are under the player's control."[17] Cuzzucoli then implements mathematical models that describe and incorporate the above five parameters.

Through empirical analysis, the many features of the guitar, such as bracing, wood choice, and body design have been studied and documented. In addition, purely mathematical studies, such as Derveaux's complete model of the guitar and Cuzzucoli's version of the model with the added player's touch, have provided many insights on the physical and tonal properties of the guitar. While much is known about guitars, the previous studies do not generalize to everybody's guitars. In addition, the above studies do not give enough information, nor is a practical approach, to determine microphone placements for an acoustic guitar.

1.2 Recording Techniques

The art of sound recording and audio engineering is a very subjective art, with more guidelines than established rules.[18] In a recording situation, the audio engineer must make decisions on how to achieve the most high-quality sound. The engineer must then make decisions on choices of room environments, instruments, microphones, microphone placements, and pre-amplifiers. In addition, the engineer must make decisions on how to use effects, such as reverbs, equalizers, and compressors, effectively to create the best possible sound. It is easy to see that many decisions fall upon the engineer, and expert knowledge on these many factors and parameters help to make decisions easier and faster. However, knowing how microphones work and suggested microphone placements act as template to help the engineer get started, and then the engineer can customize the choices to get the desired sound.

First of all, a microphone is a transducer, which "changes one form of energy (sound waves)

17 Cuzzucoli,"A Physical Model of the Classical Guitar, Including the Player's Touch," 60.
18 Huber, *Modern Recording Techniques,* 111.

into another corresponding form of energy (electrical signals)."[19] Excluding ribbon microphones, two main types of microphones exist, dynamic and condensers. A dynamic microphone consists of a diaphragm attached to a magnet, which is wrapped with a wire coil. "Whenever an acoustic pressure wave hits the diaphragm's face, the magnet is displaced in proportion to the amplitude and frequency of the wave. In doing so, an analogous electrical signal is induced into the coil and across the output leads, producing an analog output signal."[20] Condenser microphones, on the other hand, operate by having two electrically charged plates, with one connected to the diaphragm. "When sound acts upon the movable diaphragm, the varying distance between the plates will likewise create a change in the device's capacitance."[21] This change in capacitance creates a change in voltage, which creates an output signal with the respective frequency and amplitude. Therefore, microphones largely respond to pressure waves.

Pressure can be described in two ways, in pascals and in decibels. The pascal is a measurement of the change in air density from the equilibrium density at a given point in space.[22] When a sound wave moves through the air, the areas where the air is compressed has positive pascal values, since there is a positive change in air density from the equilibrium pressure. In the areas of rarefaction, the pascal value is negative, since there is a negative change in air density from the equilibrium pressure. The pascal magnitude can be seen as the amplitude of a wave. If the magnitude of pascal measurement is high, then the change in air density is high, resulting in a loud sound. However, pascal values have a big range, so the decibel was introduced to make the numbers more manageable. The equation for the decibel level, or sound pressure level (SPL), is

$$SPL = 20\log_{10}\left(\frac{P_m}{P_{ref}}\right) \quad (1),$$

19 Ibid., 111.
20 Ibid., 113.
21 Ibid., 115.
22 Lawrence E. Kinsler et al., *Fundamentals of Acoustics, Third Edition* (New York: John Wiley & Sons, 1982), 100.

where P_m is the measured pressure in pascals and $P_{ref} = 0.00002$ pascals.[23]

There are many suggested guidelines for microphone choices and placements. Usually a condenser microphone is used to mic an acoustic guitar because it has a higher transient and frequency response than a dynamic microphone, giving it the ability to pick up more of the guitar's harmonic content. In terms of distance, the engineer has two basic choices, distant miking or close miking. Distant miking is defined as a distance of 3 feet or more. David Huber, in the book Modern Recording Techniques, states that distant miking "can pick up a large portion of a musical instrument, thereby preserving the overall tonal balance of that source."[24] In addition, distant miking "allows the room's acoustic environment to be picked up with the direct sound signal."[25] In contrast, close miking is defined as a distance between 1 inch to 3 feet from a sound source. Huber states that close miking "creates a tight, present sound quality, and it effectively excludes the acoustic environment."[26]

In addition, the engineer has a decision to perform mono or stereo miking. Mono miking involves recording with only one microphone. Therefore, the engineer must place it in a spot which has the best tonal balance. In stereo miking, two main techniques are used, a spaced pair and a x/y pair. In a spaced pair, two microphones are placed in a room and spaced apart. "This technique places the two microphones anywhere from only a few feet to more than 30 feet apart and uses time and amplitude cues in order to create a stereo image."[27] However, this microphone technique has one drawback, phase issues. "The primary drawback to this technique is the strong potential for phase discrepancies between the two microphones due to the differences in the sound's arrival time at one mic relative to the other."[28] However, a x/y pair is a stereo microphone technique that does not suffer from phase problems. The x/y technique involves taking two microphones and placing their grills as close as possible, with an angle

23 Huber, *Modern Recording Techniques,* 60.
24 Ibid., 133.
25 Ibid., 133.
26 Ibid., 135.
27 Ibid., 142.
28 Ibid., 142.

between 90 and 135 degrees. “X/y stereo miking is an intensity-independent system that uses only the cue of amplitude to discriminate direction. In addition, due to their proximity, no appreciable phase problems arise.”[29] The midpoints of the two microphones are usually aimed at the sound source, and the two microphones are panned left and right to create a stereo image.

With these techniques in mind, suggested microphone placement techniques exist for the acoustic guitar. “A balanced pickup can often be achieved by placing a microphone, or a x/y pair, at a point slightly off axis to the sound-hole and above or below the sound hole at a distance of between 6 inches and 1 foot.”[30] In addition, there are spaced microphone techniques for the guitar. They usually comprise of one microphone aimed at the 12th fret and the other aimed somewhere around the bridge or lower-body.[31] These microphones are usually at a distance of 6 inches to a foot from the guitar.

1.3 My Research Contribution

Many works have been done to study guitar modes and how guitars vibrate. In addition, there are suggested guidelines for microphone placement techniques. However, different guitars have different vibrational patters; that is why different brands of guitars have different sonic characteristics. Therefore, microphone placements may change depending on what kind of guitar is used in recording sessions. In addition, modal studies performed by Dr. Russell and the mathematical models derived by Derveaux only work for observing how a guitar vibrates for one frequency. Because a guitarist usually plays chords, the way the guitar surface vibrates and radiates sound must be studied to determine optimal microphone placements. My research method is to then use the mathematical technique Near-field Acoustic Holography (NAH). NAH is a method, in contrast to previous numerical techniques, that integrates experimental data into the algorithm for predicting the acoustic pressures of a vibrating

29 Ibid., 142.
30 Ibid., 152.
31 Paul White, “Recording Acoustic Guitar,” *Sound on Sound,* August 2001, http://www.soundonsound.com/sos/aug01/articles/recacgtr0801.asp (accessed March 24, 2012).

source. This technique provides an efficient way to derive the pressures on the guitar surface and the pressures at any distance away from the guitar. By using the superposition of waves principle from physics with NAH, one can then use the data to analyze chords.

Chapter 2: Near-field Acoustic Holography (NAH)

2.1 History and Development of NAH

NAH is a powerful mathematical tool that is used to observe how a source is vibrating.[32,33,34,35] This is done by taking pressure measurements on a hologram above the surface. A hologram is defined as a fictitious two-dimensional surface surrounding a three-dimensional object of interest which contains pressure information. Then, the Helmholtz equation is used to derive the source pressures of a vibrating object. "On a fundamental level, the great utility of holography arises from its high information content, that is, data recorded on a two-dimensional surface (the hologram) may be used to reconstruct an entire three-dimensional wave field, with the well-known result of obtaining three-dimensional images."[36] Not only does NAH produce a three-dimensional wave field, other quantities can be calculated from it. "In NAH, the recording of the sound pressure field on a two-dimensional surface can be used to determine not only the three-dimensional sound pressure field but also the particle velocity field, the acoustic vector intensity field, the surface velocity field, the surface velocity and intensity of a vibrating source, etc."[37] The high content of information from only measuring points on a two-dimensional surface make NAH an efficient and valuable way to measure and predict sound

32 J.D. Maynard et al., "Nearfield Acoustic Holography: I. Theory of Generalized Holography and the Development of NAH," *Journal of the Acoustical Society of America* 78, no. 4 (1985).
33 Mingsian R. Bai, "Application of BEM (Boundary Element Method)-Based Acoustic Holography to Radiation Analysis of Sound Sources with Arbitrarily Shaped Geometries," *Journal of the Acoustical Society of America* 92, no. 1 (1992).
34 G.T. Kim et al., "3-D Sound Source Reconstruction and Field Prediction Using the Helmholtz Integral Equation," *Journal of Sound and Vibration* 136, no. 2 (1990).
35 Sean F. Wu, "Hybrid Near-field Acoustic Holography," *Journal of the Acoustical Society of America* 115, no. 1 (2004).
36 J.D. Maynard, "Nearfield Acoustic Holography: I. Theory of Generalized Holography and the Development of NAH," 1395.
37 Ibid., 1395.

radiation from a vibrating object. Techniques of implementing NAH have evolved over time, and now there exists techniques to achieve great accuracy for many types of vibrating surface domains.

NAH theory was thoroughly written and implemented in the paper "Nearfield Acoustic Holography: I. Theory of Generalized Holography and the Development of NAH," by J. D. Maynard. In this paper, Maynard states the benefits and limitations of NAH. The benefits are described in the above paragraph; however, the limitations are the following: the hologram is recorded with single frequency radiation; the hologram is recorded with a reference wave for phase information; the wavelength of the radiation limits the spatial resolution of the reconstruction; a hologram which records a specific scalar field can only be used to reconstruct that same field; a known Green's function is used; and the field being measured obeys the wave equation.[38] Maynard then develops Fourier-Transform-Based NAH. This technique is very beneficial for easy geometric surfaces, such as planes and spheres (due to symmetry principles). Maynard then implements Fourier-Transform-Based NAH by studying a vibrating two-dimensional plate using a 16x16 array of transducers to measure the hologram.[39]

Since Maynard's paper, many different mathematical techniques have been implemented to study all kinds of challenging sources. These techniques are summarized in the paper "Techniques for Implementing Near-field Acoustical Holography," by Sean Wu. Wu states that there are three main techniques to implement NAH: Fourier-Transform-Based NAH, Boundary Element Method, and the Least Squares Method. The first technique, Fourier-Transform-Based NAH, is the method developed and used by Maynard. While computationally the easiest method to implement, the main requirement is that the geometry is either planar, spherical, or cylindrical. Wu states, "In practice, few structures have a level of constant coordinates. Therefore, the Fourier-Transform-Based NAH is limited in its applications."[40]

38 Ibid., 1396-1397.
39 Ibid., 1396-1413.
40 Sean F. Wu, "Techniques for Implementing Near-Field Acoustical Holography," *Sound and Vibration,* February 2010, 13.

To handle more general geometries, Boundary Element Method-based NAH was developed. By taking the Helmholtz integral equation, discretizing the source surface, and performing the integrals in each discretized region, the boundary element method is an efficient technique to use on any general source that can be discretized. Wu states that the main advantages of the boundary element method are, "It allows for reconstruction of the acoustic quantities on an arbitrarily shaped structure, there are no restrictions on the locations of measurement points on a hologram surface as long as they conform to the contour of the target surface in a near field, there are no restrictions on the locations of reconstruction points, and it is applicable in both exterior and interior regions."[41] However, the boundary element method has one major limitation. "Since the acoustic quantities on an arbitrary surface are obtained using a spatial discretization, one must have a minimum number of nodes per wavelength to avoid distortions in reconstruction. For a complex structure such as a vehicle, the number of discrete nodes required to display surface acoustic quantities accurately may be huge."[42]

Two papers have fully described and implemented the boundary element method, "Application of Boundary-Element Method Based Acoustic Holography to Radiation Analysis of Sound Sources with Arbitrarily Shaped Geometries" by Mingsian Bai, and "3-D Sound Source Reconstruction and Field Reprediction using the Helmholtz Integral Equation" by G.T. Kim. In the first paper, Bai derives the equations for the boundary element method technique. In addition, since the Helmholtz integral equation contain singularities, Bai derives a method so that the equation contains no singularities, making the boundary element method easier to solve. Bai's method is the method I chose to use, and a full formulation is in Section 2.4. Bai then tests boundary element method-based NAH on a pulsating sphere, a pulsating cylinder with two spherical end-caps, and a vibrating piston set in a rigid sphere. This method achieved accurate results.[43] In the second paper, Kim also develops boundary element-

41 Ibid., 13.
42 Ibid., 13.
43 Bai, "Application of BEM (Boundary Element Method)-Based Acoustic Holography to Radiation Analysis of Sound Sources with Arbitrarily Shaped Geometries," 533-549.

based NAH. However, Kim focuses more on the discretization of the sound source. Kim states that to achieve the desired accuracy, the element dimensions should be less than a quarter of the wavelength of the measured frequency.[44] Kim then uses NAH to study the vibration of a speaker cabinet.[45]

The third technique used to implement NAH is the Least Squares method. According to Wu, "The least squares method, unlike the first two methods, does not seek an exact solution to the acoustic field generated by an arbitrary surface, but rather an approximation for an acoustic field using an expansion of the admissible basis functions with errors minimized by least squares."[46] While this method is simple and efficient to implement, Wu states that "the main limitation of least squares method is that there are no single set of coordinate systems that can provide a good approximation for all surface geometries."[47] In addition, Wu states in his paper "Hybrid Near-field Acoustic Holography," that "test results also indicate that the least squares method is not ideal for a highly irregular surface due to a slow convergence of the expansion solution."[48]

In addition, these methods have been combined to try to create more accurate results. This is shown in the paper "Hybrid Near-field Acoustic Holography," by Wu. In this paper, Wu combines the boundary element method and the least squares method. Wu states, "this hybrid NAH is derived from a modified least squares method, which expands the acoustic pressure in terms of outgoing and incoming waves, and combines it with the boundary element method. Both the accuracy and efficiency of reconstruction are enhanced when the least squares method converges fast on the measurement surface."[49] Wu then uses hybrid NAH to study the vibration of an engine block.

44 Kim, "3-D Sound Source Reconstruction and Field Prediction Using the Helmholtz Integral Equation," 251.
45 Ibid., 254.
46 Wu, "Techniques for Implementing Near-Field Acoustical Holography," 13.
47 Ibid., 13.
48 Wu, "Hybrid Near-field Acoustic Holography," 207.
49 Ibid., 208.

2.2 Applications of NAH

So far, NAH has been used to solve for source pressures and velocities for many objects. As previously mentioned, G. Kim used NAH for a loudspeaker cabinet, Wu used NAH on an engine block, and Maynard used NAH on a vibrating plate. NAH, therefore, has been used as a tool to evaluate radiation of sound coming from an object, and is used primarily for noise control. In a broader context, boundary integral formulations used in BEM-based NAH are used to study scattering of waves from objects. In the publications of Dr. Alex Barnett[50] and Dr. Mahadevan Ganesh[51], pressure fields formed by waves scattering from objects were studied by only discretizing the object surfaces and performing the boundary integrals.

In addition, NAH has been used to study a few musical instruments. The modes of a frame drum were studied using NAH by Gregoire Tronel.[52] In addition, a violin was studied by Lily Wang. Because the guitar and violin are in the same musical family (chordophones), it is beneficial to see what the results of the violin were. "First, the top plate was found to be the dominant source of sound energy radiation from the violin. At low frequencies, diffraction of sound radiation from the top plate around the violin body produces far-field omnidirectional radiation. At higher frequencies, the regions of energy sources become more localized and are distributed asymmetrically on the violin body."[53] In other words, different parts of the violin vibrate depending on the frequency. The guitar should do the same, meaning that different microphone techniques may have to be used if the performer is playing a variety of notes.

50 Alex Barnett et al., "A New Integral Representation for Quasi-Periodic Scattering Problems in Two Dimensions," *BIT Numerical Mathematics* 51 (2011): 67-90.

51 Mahadevan Ganesh et al., "A Fully Discrete Galerkin Method for High Frequency Exterior Acoustic Scattering in Three Dimensions," *Journal of Computational Physics* 230 (2011): 104-125.

52 Gregoire Tronel, "Near-field Acoustic Holography: The Frame Drum," (Powerpoint Presentation, University of Illinois at Urbana-Champaign, 2010)

53 Lily M. Wang et al., "Acoustic Radiation from Bowed Violins," *Journal of the Acoustical Society of America* 110, no. 1 (2001): 554.

2.3 Benefits of NAH

Without NAH, two approaches could be implemented to perform my research. The first approach is to empirically observe how my guitar vibrates using the methods of Dr. Russell. The second approach is to use mathematical models, like Derveaux, and adjust the equation parameters to those of my guitar. I decided not to use empirical methods because that requires the use of specific and expensive laboratory equipment. In order for my method to be adopted into the music industry, a cost-effective approach must be taken. I also decided not to use Derveaux's method because the calculations are very laborious, and Derveaux had to make many assumptions. I decided to use NAH because by measuring pressures on a hologram, source pressures can be found. In addition, this data is unique to my guitar. NAH can also calculate pressure fields at any point surrounding the guitar. Therefore, any combination of close miking and distant miking positions can be found.

In reviewing all of the techniques of NAH, Dr. Sussman and I have agreed that the boundary element method is the best for our situation. We chose the boundary element method because only the mesh of the boundary is required, not a volume mesh, thus reducing the dimension size of the problem by 1. This technique also works well with arbitrary, difficult domains, like the surface of a guitar. We decided not to do the least squares method, which also reduces the dimension by 1, because the guitar body contains irregularities, such as sharp corners, curved surfaces, and a sound-hole on the top plate, so it would be more prone to convergence problems.[54]We also decided to not do any of the hybrid boundary element-least squares techniques because, in analyzing the methods, the degree of accuracy gained is not worth the computational cost of the added steps. The boundary element method should give us accurate results already, since we are dealing with relatively low frequency sounds, which are easier to get high resolution results than higher frequencies. Specifically, the main technique that I implemented is from Bai's paper. The main advantage of using his boundary element method-based

54 Wu, “Hybrid Near-field Acoustic Holography,” 207.

NAH is that he creates a system of equations in matrix form, which is easy to program, and the integrands do not contain singularities, which make integration techniques easy to implement.

2.4 Formulation of NAH

The equations for NAH are derived from the wave equation,

$$u_{tt} = c^2 \nabla^2 u \quad (2)$$

where c is the speed of the wave. Assuming that u is separable,

$$u = p(\vec{x}) T(t) \quad (3)$$

the separation of variables technique can be used to solve the wave equation. Plugging in eq.(3) into the wave equation, eq.(2), gives

$$p(\vec{x}) T''(t) = c^2 \nabla^2 p(\vec{x}) T(t) \quad (4).$$

Simplifying gives

$$\frac{T''(t)}{c^2 T(t)} = \frac{\nabla^2 p(\vec{x})}{p(\vec{x})} = -k^2 \quad (5).$$

Solving for $T(t)$ gives a second-order ordinary differential equation,

$$T''(t) + \omega^2 T(t) = 0 \quad \text{, where} \quad \omega = kc \quad (6).$$

Solving gives

$$T(t) = Ae^{i\omega t} + Be^{-i\omega t} \quad (7).$$

This means that T is time-periodic. Solving for $p(x)$ gives

$$\nabla^2 p(\vec{x}) + k^2 p(\vec{x}) = 0 \quad \text{where} \quad k = \frac{\omega}{c} \quad (8).$$

k is called the wavenumber. Eq.(8) is called the Helmholtz equation, and is the main equation for NAH.

Because u in eq.(2) is time-periodic, the Helmholtz equation can also be derived from the wave equation by using the frequency-time Fourier transform pair. The Fourier transform pair is

$$\hat{u}(x,y,z,\omega)=\int_{-\infty}^{\infty} u(x,y,z,t)e^{i\omega t}dt \quad (9) \text{ and } \quad u(x,y,z,t)=\frac{1}{2\pi}\int_{-\infty}^{\infty} \hat{u}(x,y,z,\omega)e^{-i\omega t}d\omega \quad (10).$$

By substituting eq.(10) into the wave equation, eq.(2), one derives

$$\frac{1}{2\pi}\int_{-\infty}^{\infty} \nabla^2\hat{u}(x,y,z,\omega)e^{-i\omega t}d\omega-\frac{1}{2\pi c^2}\int_{-\infty}^{\infty}\frac{\partial^2}{\partial t^2}[\hat{u}(x,y,z,\omega)e^{-i\omega t}]d\omega=0 \quad (11)$$

By simplifying and taking the second partial derivative with respect to time in the second integral, one then derives

$$\frac{1}{2\pi}\int_{-\infty}^{\infty} e^{-i\omega t}(\nabla^2\hat{u}(x,y,z,\omega)+\frac{\omega^2}{c^2}\hat{u}(x,y,z,\omega))d\omega=0 \quad (12)$$

In order for the integral to equal zero, the integrand must be zero, giving

$$\nabla^2\hat{u}(x,y,z,\omega)+k^2\hat{u}(x,y,z,\omega)=0 \quad \text{where} \quad k=\frac{\omega}{c} \quad (13),$$

which is the Helmholtz Equation, eq.(8).

In NAH, the exterior Helmholtz equation is solved,

$$\nabla^2 p+k^2 p=0 \quad \text{in} \quad +\Omega \quad (14),$$

where Ω is the volume enclosed by the surface Γ and with Dirichlet conditions,

$$u(x,y,z)=\bar{u} \quad \text{on} \quad \Gamma \quad (15).$$

In order to solve the Helmholtz equation for exterior domains a condition on the solution is imposed,

$$\lim_{r\to\infty} r(\frac{\partial p}{\partial r}+ikp)=0 \quad (16).$$

This is called the Sommerfeld Radiation condition.[55] This condition forces the solution, p, to approach zero as the waves get farther from the source (as r approaches infinity).

To understand how the solutions to the Helmholtz equation behave, it is beneficial to solve the equation in different dimensions. In one dimension, the Helmholtz equation is

$$\frac{d^2 p}{dx^2}+k^2 p=0 \quad (17).$$

55 Bai, "Application of BEM-Based Acoustic Holography," 534.

The characteristic equation to solve this 2nd order homogenous ordinary differential equation is

$$\lambda^2+k^2=0 \quad \text{and} \quad \lambda=\pm ik \quad (18).$$

So, the solution to the 1-D Helmholtz equation is $p(x)=Ae^{ikx}+Be^{-ikx}$ (19), where A and B are constants. If we assume that $p(x)$ is a simple wave and that B = 0, A is the amplitude of the wave and the wavenumber k has a control over the frequency of the wave. By placing $p(x)$ into eq.(3), and assuming that A=0 in the time equation, T, the solution to the wave equation becomes

$$u(x,t)=Ae^{i(kx-\omega t)} \quad (20).$$

By taking the real part of u in eq.(20),

$$u(x,t)=A\cos(kx-\omega t) \quad (21).$$

This solution is a traveling wave.

The Helmholtz equation in 2 dimensions is $\nabla^2 p+k^2 p=0$, where the laplacian operator is

$$\nabla^2=\frac{\partial^2}{\partial x^2}+\frac{\partial^2}{\partial y^2} \quad (22).$$

It is natural to solve this equation in polar coordinates. Making the transformations,

$$x=r\cos\theta \quad \text{and} \quad y=r\sin\theta \quad (23),$$

differentiation and the chain rule is used to derive the laplacian in polar coordinates.

$$\frac{\partial p}{\partial x}=\frac{\partial p}{\partial r}\frac{\partial r}{\partial x}+\frac{\partial p}{\partial \theta}\frac{\partial \theta}{\partial x} \quad (24)$$

$$\frac{\partial^2 p}{\partial x^2}=\frac{\partial p}{\partial r}\frac{\partial^2 r}{\partial x^2}+\frac{\partial r}{\partial x}\left(\frac{\partial^2 p}{\partial r^2}+\frac{\partial^2 p}{\partial r\,\partial \theta}\right)+\frac{\partial^2 \theta}{\partial x^2}\frac{\partial p}{\partial \theta}+\frac{\partial \theta}{\partial x}\left(\frac{\partial^2 p}{\partial r\,\partial \theta}+\frac{\partial^2 p}{\partial \theta^2}\right) \quad (25)$$

Similarly,

$$\frac{\partial p}{\partial y}=\frac{\partial p}{\partial r}\frac{\partial r}{\partial y}+\frac{\partial p}{\partial \theta}\frac{\partial \theta}{\partial y} \quad (26)$$

$$\frac{\partial^2 p}{\partial y^2}=\frac{\partial p}{\partial r}\frac{\partial^2 r}{\partial y^2}+\frac{\partial r}{\partial y}\left(\frac{\partial^2 p}{\partial r^2}+\frac{\partial^2 p}{\partial r\,\partial \theta}\right)+\frac{\partial^2 \theta}{\partial y^2}\frac{\partial p}{\partial \theta}+\frac{\partial \theta}{\partial y}\left(\frac{\partial^2 p}{\partial r\,\partial \theta}+\frac{\partial^2 p}{\partial \theta^2}\right) \quad (27).$$

The partial differential equations necessary to solve the above equation are

$$\frac{\partial r}{\partial x}=\frac{x}{r} \quad , \quad \frac{\partial^2 r}{\partial x^2}=\frac{1}{r}-\frac{x^2}{r^3}=\frac{x^2+y^2-x^2}{r^3}=\frac{y^2}{r^3} \quad (28),$$

$$\frac{\partial r}{\partial y}=\frac{y}{r} \quad , \quad \frac{\partial^2 r}{\partial y^2}=\frac{1}{r}-\frac{y^2}{r^3}=\frac{x^2+y^2-y^2}{r^3}=\frac{x^2}{r^3} \quad (29),$$

$$\frac{\partial \theta}{\partial x}=\frac{-y}{r^2} \quad , \quad \frac{\partial^2 \theta}{\partial x^2}=\frac{2xy}{r^4} \quad (30),$$

$$\frac{\partial \theta}{\partial y}=\frac{x}{r^2} \quad , \quad \frac{\partial^2 \theta}{\partial y^2}=\frac{-2xy}{r^4} \quad (31).$$

By plugging the above partials into $\frac{\partial^2 p}{\partial x^2}$ and $\frac{\partial^2 p}{\partial y^2}$ and adding the two terms, many cancelations result and the laplacian operator becomes

$$\nabla^2 p=\frac{\partial^2 p}{\partial r^2}+\frac{1}{r}\frac{\partial p}{\partial r}+\frac{1}{r^2}\frac{\partial^2 p}{\partial \theta^2} \quad (32).$$

So, the 2-D Helmholtz equation becomes

$$\frac{\partial^2 p}{\partial r^2}+\frac{1}{r}\frac{\partial p}{\partial r}+\frac{1}{r^2}\frac{\partial^2 p}{\partial \theta^2}+k^2 p=0 \quad (33).$$

Using separation of variables, $P(r,\theta)=R(r)\Theta(\theta)$, the 2-D Helmholtz equation becomes

$$R''(r)\Theta(\theta)+\frac{1}{r}R'(r)\Theta(\theta)+\frac{1}{r^2}R(r)\Theta''(\theta)+k^2 R(r)\Theta(\theta)=0 \quad (34).$$

Dividing by $R(r)\Theta(\theta)$ and separating the two functions, the above equation becomes

$$\frac{\Theta''(\theta)}{\Theta(\theta)}=\frac{-r^2}{R(r)}\left(R''(r)+\frac{1}{r}R'(r)\right)-r^2k^2=-\gamma^2 \quad (35).$$

The theta equation is a 2nd order ordinary differential equation,

$$\Theta''(\theta)+\gamma^2\Theta(\theta)=0 \quad (36),$$

and has a periodic solution,

$$\Theta(\theta)=Ae^{i\gamma\theta}+Be^{-i\gamma\theta} \quad (37),$$

where A and B are constants. To solve the nonlinear R equation, a substitution variable, $\rho = kr$, is introduced, making the R derivatives $R_r(r) = R_\rho \frac{d\rho}{dr} = k\, R_\rho$ (38) and $R_{rr}(r) = k^2 R_{\rho\rho}$ (39). Plugging in the substitutions give Bessel's differential equation,

$$R_{\rho\rho} + \frac{1}{\rho} R_\rho + \left(1 - \frac{\gamma^2}{\rho^2}\right) R = 0 \quad (40).$$

This differential equation has a special solution called the Bessel function, written as $J_\gamma(\rho)$.[56] The Bessel function behaves very much like a damped cosine wave. The amplitude of the wave approaches 0 as ρ approaches infinity (which happens as r approaches infinity).

To visualize the complete solution of the 2-D Helmholtz equation, it is easy to imagine a stretched circular membrane, like a drum head, that has been struck with a beater. The R equation prescribes outward propagating waves from the beater, where the amplitude of the wave decays to zero as the wave gets farther from the beater. In addition, the theta equation makes the R waves oscillate around the beater. The two dimensional case is very interesting because not only are there waves propagating outward, but the waves are moving in a circular direction around the beater.

The Helmholtz equation in 3 dimensions also has some interesting properties. By making the substitutions

$$x = r\sin\theta\cos\phi \quad , \quad y = r\sin\theta\sin\phi \quad , \quad z = r\cos\theta \quad (41),$$

and using the same techniques as the 2-D case, the Helmholtz equation becomes

$$p_{rr} + \frac{2}{r} p_r + \frac{1}{r^2}\left[\frac{1}{\sin^2\theta} p_{\phi\phi} + \frac{1}{\sin\theta}(\sin\theta\, p_\theta)_\theta\right] + k^2 p = 0 \quad (42).$$

Separating only the r variable, $p = R(r)\, Y(\theta, \phi)$, the 3-D Helmholtz equation then becomes,

56 Walter A. Strauss, *Partial Differential Equations: An Introduction, Second Edition,* (New Jersey: John Wiley & Sons, 2008), 267.

$$k^2 r^2 + \frac{r^2 R_{rr}(r) + 2r R_r(r)}{R(r)} = -1 \frac{(\frac{1}{\sin^2\theta}) Y_{\phi\phi}(\theta,\phi) + (\frac{1}{\sin\theta})(\sin\theta\, Y_\theta(\theta,\phi))_\theta}{Y(\theta,\phi)} = -\gamma^2 \quad (43)^{57}$$

The R equation is then

$$R_{rr} + \frac{2}{r} R_r + (k^2 - \frac{\gamma}{r^2}) R = 0 \quad (44).$$

This equation is very similar to Bessel's equation. By making the substitution

$$w(r) = \sqrt{r}\, R(r) \quad (45),$$

the R equation then becomes

$$w_{rr} + \frac{1}{r} w_r + (k^2 - \frac{\gamma + \frac{1}{4}}{r^2}) w = 0 \quad (46).$$

The solution is Bessel's equation of order $\sqrt{\gamma + \frac{1}{4}}$, and is written $J_{\sqrt{\gamma+\frac{1}{4}}}(kr)$.[58] Therefore the solution to the R equation is

$$R(r) = \frac{J_{\sqrt{\gamma+\frac{1}{4}}}(kr)}{\sqrt{r}} \quad (47).$$

To solve the Y equation, Y is separated into $Y(\theta,\phi) = \Theta(\theta)\Phi(\phi)$. Y becomes

$$\frac{\Phi''(\phi)}{\Phi(\phi)} = -(\frac{\sin\theta(\sin\theta\Theta(\theta))_\theta}{\Theta(\theta)} + \gamma\sin^2\theta) = -\alpha^2 \quad (48).$$

The theta equation is then

$$\frac{(\sin\theta\Theta(\theta))_\theta}{\sin\theta} + (\gamma - \frac{\alpha^2}{\sin^2\theta})\Theta(\theta) = 0 \quad (49).$$

This equation also has a special solution, called the Legendre function, written

$$\Theta(\theta) = P_l^\alpha(\cos\theta) \quad (50).^{59}$$

57 Ibid., 271.
58 Ibid., 272.
59 Ibid., 273.

This function is a polynomial that acts like the cosine function, and is harmonic. $\Phi(\phi)$ is a 2nd order homogeneous ordinary differential equation

$$\Phi(\phi)+\alpha^2\Phi(\phi)=0 \quad (51).$$

The solution is

$$\Phi(\phi)=Ae^{i\alpha\phi}+B\,e^{-i\alpha\phi} \quad (52).$$

If we assume that B = 0 in eq.(52), the full solution to the 3-dimensional Helmholtz equation is

$$p(r,\theta,\phi)=\frac{J_{l+\frac{1}{2}}(kr)}{\sqrt{r}}P_l^{\alpha}(\cos\theta)e^{i\alpha\phi} \quad (53).$$

It is very interesting to note that the waves oscillates around the sphere, (θ,ϕ), in addition to outward propagating waves. Also, the pressure becomes zero as r approaches infinity, satisfying the Sommerfeld Radiation condition, eq.(16).

The above solutions to the 1-D, 2-D, and 3-D Helmholtz equations are over simple geometries. However, the guitar is not a simple geometric shape. Therefore, it is appropriate to use numerical approximation techniques to solve the Helmholtz equation. The approximation technique that will be used is the boundary element method. The boundary element method is preferred over other techniques, such as the finite element method, because the boundary element method takes a 3 dimensional problem and reduces it to a 2 dimensional problem. Utilizing Green-Gauss' theorem, the boundary element method applied to the Helmholtz equation states that if the solution and the solution gradient on the surface of a vibrating object is known, then solutions can be calculated anywhere around the surface of the vibrating object. This is an extremely powerful statement because pressures can be calculated for any point outside of the guitar body, and is one of the main motivating factors for choosing the boundary element method. Two steps are used to implement the boundary element method. First, the Helmholtz equation is multiplied by a weighting function and transformed to an

integral problem. Then the source surface is discretized into triangular elements and the integrals are performed on each triangle.

First, a weighting function is chosen. The weighting function, W, is chosen such that it satisfies the inhomogeneous point-source Helmholtz equation,

$$\nabla^2 W + k^2 W = \delta(\xi - x, \eta - y, \zeta - z) \quad (54).^{60}$$

The delta function, $\delta_\epsilon(x, y, z)$, is defined as a function which is constant within a sphere of radius ϵ centered at the origin, zero outside the sphere, and $\int \delta_\epsilon = 1$. Then the Dirac delta function is

$$\delta(x, y, z) = \lim_{\epsilon \to 0} \delta_\epsilon \quad (55)$$

The Dirac delta function, $\delta(\xi - x, \eta - y, \zeta - z)$, has some interesting properties

$$\delta(\xi - x, \eta - y, \zeta - z) = 0 \quad \text{if} \quad (x, y, z) \neq (\xi, \eta, \zeta) \quad \text{, and}$$

$$\delta(\xi - x, \eta - y, \zeta - z) = \infty \quad \text{if} \quad (x, y, z) = (\xi, \eta, \zeta) \quad (56).$$

Because of these properties, the Dirac delta function has the property that if $(\xi, \eta, \zeta) \in \Omega$,

$$\iiint_\Omega \delta(\xi - x, \eta - y, \zeta - z)\, d\Omega = 1 \quad (57),$$

and if $(\xi, \eta, \zeta) \notin \Omega$,

$$\iiint_\Omega \delta(\xi - x, \eta - y, \zeta - z)\, d\Omega = 0 \quad (58).^{61}$$

Therefore, in order to find a W which satisfies eq.(54), two conditions must be met: W must be a function that satisfies the homogeneous Helmholtz equation; and W must contain a singularity at the point (ξ, η, ζ) .[62]

To find W, a local coordinate system is then adopted around the singular point

60 Peter Hunter, "FEM/BEM Notes," (New Zealand: The University of Auckland, Department of Engineering Science, 1997), 46.
61 Ibid., 43-45.
62 Ibid., 46.

$$r=\sqrt{(\xi-x)^2+(\eta-y)^2+(\zeta-z)^2} \quad (59).^{63}$$

The Helmholtz equation is then transformed as in the 3-D case,

$$W_{rr}+\frac{2}{r}W_r+\frac{1}{r^2}[W_{\theta\theta}+(\cot\theta)W_\theta+\frac{1}{\sin^2\theta}W_{\theta\theta}]+k^2W=\delta(\xi-r\sin\theta\cos\phi,\eta-r\sin\theta\sin\phi,\zeta-r\cos\theta)$$
(60).

Because of symmetry about the singular point, W_θ , $W_{\theta\theta}$, and $W_{\phi\phi}$ are all zero, making eq.(60) only dependent on r. For r > 0, $\delta(\xi-x,\eta-y,\zeta-z)=0$ and eq.(60) becomes

$$W_{rr}+\frac{2}{r}W_r+k^2W=0 \quad (61).$$

The solution for this equation is

$$W=\frac{e^{ikr}}{4\pi r} \quad (62).^{64}$$

This solution can be easily shown to solve eq.(61) when r > 0,

$$W_r=\frac{ike^{ikr}}{r}-\frac{e^{ikr}}{r^2} \quad , \quad W_{rr}=\frac{-k^2e^{ikr}}{r}-\frac{2ike^{ikr}}{r^2}+\frac{2e^{ikr}}{r^3} \quad (63).$$

Plugging in the above derivatives give

$$\frac{-k^2e^{ikr}}{r}-\frac{2ike^{ikr}}{r^2}+\frac{2e^{ikr}}{r^3}+\frac{2ike^{ikr}}{r^2}-\frac{2e^{ikr}}{r^3}+\frac{k^2e^{ikr}}{r}=0 \quad (64).$$

Also, $\iiint_\Omega (W_{rr}+\frac{2}{r}W_r+k^2W)\,d\Omega=1$ when W is given by eq.(62). Therefore, the two conditions are satisfied for W, making W a valid solution for eq.(54), and a proper weighting function. In addition, W satisfies the Sommerfeld Radiation condition because $W\to0$ and $\frac{\partial W}{\partial r}\to0$ as $r\to\infty$.

63 Ibid., 46.
64 Bai, "Application of BEM-Based Acoustic Holography," 534.

The boundary integral formulation of the Helmholtz equation is found by multiplying eq.(14) by W and triple integrating both sides over the exterior region $+\Omega$.

$$\iiint_{+\Omega} \nabla^2 p\, W\, d\Omega + \iiint_{+\Omega} k^2\, p\, W\, d\Omega = 0 \quad (65).$$

The Green-Gauss Theorem, which is the multi-integral equivalent to integration by parts,

$$\int_{\Omega} (f\, \nabla\cdot\nabla g + \nabla f\cdot\nabla g)\, d\Omega = \int_{\Gamma} f\, \frac{\partial g}{\partial n}\, d\Gamma \quad (66),^{65}$$

is used on the first triple integral in eq.(65).

$$\iint_{\Gamma} \frac{\partial p}{\partial n} W\, d\Gamma - \iiint_{+\Omega} \nabla p \nabla W\, d\Omega + \iiint_{+\Omega} k^2\, p\, W\, d\Omega = 0 \quad (67).$$

Using Green-Gauss theorem again on the second integral in eq.(67) gives

$$\iint_{\Gamma} \frac{\partial p}{\partial n} W\, d\Gamma - \iint_{\Gamma} \frac{\partial W}{\partial n}\, p\, d\Gamma + \iiint_{+\Omega} \nabla^2 W\, p\, d\Omega + \iiint_{+\Omega} k^2\, p\, W\, d\Omega = 0 \quad (68).$$

Combining the last two triple integrals in eq.(68) give

$$\iint_{\Gamma} \frac{\partial p}{\partial n} W\, d\Gamma - \iint_{\Gamma} \frac{\partial W}{\partial n}\, p\, d\Gamma + \iiint_{+\Omega} (\nabla^2 W\, p + k^2\, p\, W)\, d\Omega = 0 \quad (69).$$

The last integral in eq.(69) is

$$\iiint_{+\Omega} p(\nabla^2 W + k^2 W)\, d\Omega \quad (70).$$

However, because of eq.(57), the integral becomes

$$\iiint_{+\Omega} p\, \delta(\xi - x, \eta - y, \zeta - z) = p(\xi, \eta, \zeta) \quad (71).$$

Therefore, the Helmholtz equation becomes

$$p(\xi, \eta, \zeta) = \iint_{\Gamma} \frac{\partial W}{\partial n}\, p\, d\Gamma - \iint_{\Gamma} \frac{\partial p}{\partial n} W\, d\Gamma \quad (72).$$

This is the Helmholtz integral equation.

Numerical techniques are then employed to solve eq.(72). The surface of the guitar, Γ , is discretized

65 Hunter, "FEM/BEM Notes," 33.

into triangular elements, where

$$p \equiv \sum_{\alpha}^{N} \phi_{\alpha} p_{\alpha} \quad \text{and} \quad \frac{\partial p}{\partial n} \equiv \sum_{\alpha}^{N} \phi_{\alpha} \frac{\partial p_{\alpha}}{\partial n} \quad (73).^{66}$$

p and $\frac{\partial p}{\partial n}$ are the pressure and pressure gradient values on the surface, and p_{α} and $\frac{\partial p_{\alpha}}{\partial n}$ are the pressure and pressure gradient values on the nodes α of the triangles (constants). The linear basis functions, ϕ_{α}, are defined as

$$\phi_{\alpha} = \sum_{j}^{n} \Phi_{j}(x) \phi_{j,\alpha}(x) \quad (74),$$

where $\Phi_{j}(x) = 0$ if x is outside of triangle j, and $\Phi_{j}(x) = 1$ if x is inside the triangle j. Therefore, $\phi_{\alpha} = 1$ at node α and $\phi_{\alpha} = 0$ at the other nodes.

To solve the integrals in eq.(72), each triangle is transformed from (x, y, z) space to (x', y', z') space. This is done by forming a tetrahedron with the surface triangle as the base and the unit outward normal point from the first point of the triangle as the top of the tetrahedron. The cartesian tetrahedron is then transformed to a tetrahedron in (x', y', z') space with the coordinates (0,0,0), (1,0,0), (1,1,0), (0,0,1).

Assuming that

$$x' = a_1 x + b_1 y + c_1 z + d_1$$

$$y' = a_2 x + b_2 y + c_2 z + d_2$$

$$z' = a_3 x + b_3 y + c_3 z + d_3 \quad (75),$$

the resulting matrix system is used to determine the coefficients of the transformation

$$\begin{pmatrix} A_x & A_y & A_z & 1 \\ B_x & B_y & B_z & 1 \\ C_x & C_y & C_z & 1 \\ D_x & D_y & D_z & 1 \end{pmatrix} \begin{pmatrix} a_1 & a_2 & a_3 \\ b_1 & b_2 & b_3 \\ c_1 & c_2 & c_3 \\ d_1 & d_2 & d_3 \end{pmatrix} = \begin{pmatrix} 0 & 0 & 0 \\ 1 & 0 & 0 \\ 1 & 1 & 0 \\ 0 & 0 & 1 \end{pmatrix} \quad (76),$$

66 Ibid., 53.

where the cartesian tetrahedron nodal points are

$(A_x, A_y, A_z), (B_x, B_y, B_z), (C_x, C_y, C_z), (D_x, D_y, D_z)$. (D_x, D_y, D_z) is the unit outward normal from the point A and is found by taking the cross product of the two vectors AB and AC and normalizing.

By setting $z'=0$, one can derive (x, y, z) in terms of x' and y' , resulting in the surface integrals

$$\begin{aligned} p(x_i, y_i, z_i) = \sum_{j=1}^{J} \sum_{\alpha=1}^{N} p_\alpha \int_0^1 \int_0^{x'} \phi_{j,\alpha}(x(x', y', 0), y(x', y', 0), z(x', y', 0)) \\ \frac{\partial W_i(x(x', y', 0), y(x', y', 0), z(x', y', 0))}{\partial n} |J_j| dy' dx' \\ -\sum_{j=1}^{J} \sum_{\alpha=1}^{N} \frac{\partial p_\alpha}{\partial n} \int_0^1 \int_0^{x'} \phi_{j,\alpha}(x(x', y', 0), y(x', y', 0), z(x', y', 0)) \\ W_i(x(x', y', 0), y(x', y', 0), z(x', y', 0)) |J_j| dy' dx' \end{aligned} \quad (77)$$

where $W_i(x, y, z) = \frac{e^{ikr_i}}{4\pi r_i}$, and

$$r_i = \sqrt{(x_i - x(x', y', 0))^2 + (y_i - y(x', y', 0))^2 + (z_i - z(x', y', 0))^2} \quad (78).$$

The Jacobian, $|J|$, can be derived by the fact that the area of the pre-transformed triangle in (x, y, z) space equals the surface integral of the Jacobian over the region of the transformed triangle in (x', y') space,

$$\int_0^1 \int_0^{x'} |J| dy' dx' = Area \quad (79).$$

The Jacobian is a constant in this case, so it can be pulled out of the integrand. The double integral can then be easily solved to figure out the Jacobian.

$$|J| \int_0^1 \int_0^{x'} dy' dx' = Area$$

$$|J|\int_0^1 x'\,dx' = Area$$

$$\frac{|J|}{2} = Area$$

$$|J| = 2\cdot Area \quad (80)$$

Therefore, the Jacobian is equal to twice the area of the pre-transformed triangle.

If there are N nodes on the surface, and one solves eq.(77) for N points, one can create a system of equations and form the following matrix equation,

$$U^{ext} = D^{S,ext} * P_S - S^{S,ext} * Q_S \quad (81),$$

where U^{ext} is a Nx1 matrix containing the solution values p at (x_i, y_i, z_i) on the hologram (exterior) surface. The superscript S,ext in the D and S matrices denote that the integrals are being performed on the source surface, and the r variable in W and $\frac{\partial W}{\partial n}$ is the distance between the evaluated surface point and the exterior point of interest. Specifically, $D^{S,ext}$ is a NxN matrix containing

$$D_{i,\alpha}^{S,ext} = \sum_{j=1}^{J} \int_0^1 \int_0^{x'} \phi_{j,\alpha}(x(x',y',0), y(x',y',0), z(x',y',0)) \frac{\partial W_i(x(x',y',0), y(x',y',0), z(x',y',0))}{\partial n} |J_j|\,dy'\,dx' \quad (82)$$

P_S is a Nx1 matrix containing the surface pressure values p_α, $S^{S,ext}$ is a NxN matrix containing

$$S_{i,\alpha}^{S,ext} = \sum_{j=1}^{J} \int_0^1 \int_0^{x'} \phi_{j,\alpha}(x(x',y',0), y(x',y',0), z(x',y',0)) W_i(x(x',y',0), y(x',y',0), z(x',y',0))|J_j|\,dy'\,dx' \quad (83)$$

and Q_S is a Nx1 matrix containing the surface velocity values $\frac{\partial p_\alpha}{\partial n}$.

It is important that the number of points solved for is the same as the number of points on the surface because some matrices must be inverted at later steps, and therefore the matrices must be square.

To investigate what each element contains in the matrices $D^{S,ext}$ and $S^{S,ext}$, a simple example discretization of a surface is studied, focused at the node $\alpha = p_2$.

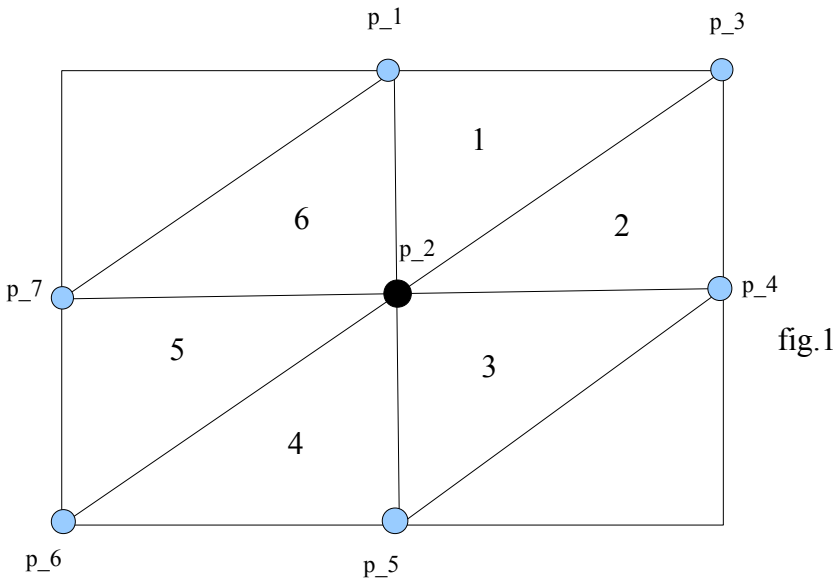

fig.1

The linearized boundary elements of each triangle are assumed to have the form

$\phi_{j,\alpha} = ax + by + cz + d$, $\phi_{j,\alpha}(p_2) = 1$ and $\phi_{j,\alpha} = 0$ (84) for the other nodes.

A basis function can then be defined for each triangular region by solving a matrix system. For example, in region 1 (j=1),

$$\phi_{1,2}(p_2) = 1$$

$$\phi_{1,2}(p_1) = 0$$

$$\phi_{1,2}(p_3) = 0$$

$$\phi_{1,2}(\acute{p}_2) = 0 \quad (85),$$

where $\acute{p}_2$ is the unit outward normal point from p_2. The above equations can be written in a

matrix system to solve for the coefficients a,b,c,d in eq.(84)

$$\begin{pmatrix} p_{2x} & p_{2y} & p_{2z} & 1 \\ p_{1x} & p_{1y} & p_{1z} & 1 \\ p_{3x} & p_{3y} & p_{3z} & 1 \\ p'_{2x} & p'_{2y} & p'_{2z} & 1 \end{pmatrix} \begin{pmatrix} a \\ b \\ c \\ d \end{pmatrix} = \begin{pmatrix} 1 \\ 0 \\ 0 \\ 0 \end{pmatrix} \quad (86).$$

Each region that has p_2 as a nodal point is then transformed to (x', y', z') space using eqns. (75-76). Therefore, the resulting matrix elements for row 2 and column i are the summation of the surface integrals over the triangles.

$$D_{i,2}^{S,ext} = \int_0^1 \int_0^{x'} \phi_{1,2} \frac{\partial W_i}{\partial n} |J_1| + \phi_{2,2} \frac{\partial W_i}{\partial n} |J_2| + \phi_{3,2} \frac{\partial W_i}{\partial n} |J_3| + \phi_{4,2} \frac{\partial W_i}{\partial n} |J_4| + \phi_{5,2} \frac{\partial W_i}{\partial n} |J_5| + \phi_{6,2} \frac{\partial W_i}{\partial n} |J_6| \, dy' \, dx' \quad (87)$$

The variable r in $\frac{\partial W}{\partial n}$ is defined as in eq.(78).

Similarly,

$$S_{i,2}^{S,ext} = \int_0^1 \int_0^{x'} \phi_{1,2} W_i |J_1| + \phi_{2,2} W_i |J_2| + \phi_{3,2} W_i |J_3| + \phi_{4,2} W_i |J_4| + \phi_{5,2} W_i |J_5| + \phi_{6,2} |J_6| W_i \, dy' \, dx' \quad (88).$$

To numerically solve the integrals in eq.(77), the functions W and $\frac{\partial W}{\partial n}$ are separated into their real and imaginary parts.

$$W = \frac{e^{ikr}}{4\pi r} = \frac{1}{4\pi} \left(\frac{\cos(kr)}{r} + i \frac{\sin(kr)}{r} \right) \quad (89)$$

Using the chain rule, $\frac{\partial W}{\partial n} = \frac{\partial W}{\partial r} \frac{\partial r}{\partial n}$,

$$\frac{\partial w}{\partial r} = \frac{1}{4\pi} \left(\frac{-\cos(kr)}{r^2} - \frac{k \sin(kr)}{r} - i \frac{\sin(kr)}{r^2} + i \frac{k \cos(kr)}{r} \right) \quad (90)$$

and

$$\frac{\partial r}{\partial n}=\nabla r\cdot\hat{n}=\frac{(x(x',y',0)-x_i)A_x}{r}+\frac{(y(x',y',0)-y_i)A_y}{r}+\frac{(z(x',y',0)-z_i)A_z}{r} \quad (91)$$

where $\hat{n}=A_x\hat{\boldsymbol{i}}+A_y\hat{\boldsymbol{j}}+A_z\hat{\boldsymbol{k}}$ and is the unit outward normal vector to the current triangle j being integrated.[67]

Because the real and imaginary parts can be linearly separated from eqns.(89-91), it is beneficial to carry out the matrix equation eq.(81), twice, one for the real part and one for the imaginary part. The answers can be combined to form the solution, i.e.

$$U_I^{real}=D^{real}*P_S-S^{real}*Q_S \quad \text{and} \quad U_I^{img}=D^{img}*P_S-S^{img}*Q_S \quad (92),$$

where the solution to the Helmholtz equation at the point (x_i,y_i,z_i) is $p(x_i,y_i,z_i)=U_I^{real}+U_I^{img}$. Eqns.(89-91) can then be substituted into the integrals in eq.(77) and calculated using Gaussian Quadrature.

Gaussian Quadrature can be used to solve a general double integral

$$F(x,y)=\int_a^b\int_{c(x)}^{d(x)}f(x,y)\,dy\,dx \quad (93).$$

Define

$$x_i=\frac{(a-b)}{2}r_i+\frac{(a+b)}{2} \quad (94)$$

and

$$y_j=(\frac{d(x_i)-c(x_i)}{2})r_j+(\frac{d(x_i)+c(x_i)}{2}) \quad (95).$$

Then the Gaussian Quadrature equation to solve eq.(93) is

67 Ibid., 58.

$$F(x,y)=\left(\frac{b-a}{2}\right)\left(\sum_{i=1}^{m}\left(\frac{d(x_i)-c(x_i)}{2}\right)c_i\left(\sum_{j=1}^{n}c_j f(x_i,y_j)\right)\right) \quad (96),$$

To achieve the most accurate approximation, 25-point Gaussian Quadrature was chosen $(m=n=5)$, with

$$\begin{aligned} r_1&=0.9061798459\\ r_2&=0.5384693101\\ r_3&=0.0000000000\\ r_4&=-0.5384693101\\ r_5&=-0.9061798459 \end{aligned}$$

$$\begin{aligned} c_1&=0.2369268850\\ c_2&=0.4786286705\\ c_3&=0.5688888889\\ c_4&=0.4786286705\\ c_5&=0.2369268850 \end{aligned} \qquad (97).^{68}$$

Because the pressures are being measured on a holographic surface above the source, the values for the matrix U^{ext} in eq.(81) are known. However, there are two unknowns, P_S and Q_S, so a constraint equation is required to find both matrices. Using the property of the Dirac delta function described in eq.(58), a fictitious surface is created in the domain $-\Omega$ such that it closely conforms to the surface. Because the exterior Helmholtz equation is not defined in this region, the Dirac delta function is zero. Therefore the matrix $U^{interior}$ is zero, creating the constraint equation,

$$0=D^{S,interior}P_S-S^{S,interior}Q_S \quad , \quad D^{S,interior}P_S=S^{S,interior}Q_S \quad (98)$$

where $D^{S,interior}$ and $S^{S,interior}$ are derived in the same manner as $D^{S,ext}$ and $S^{S,ext}$ in eq.(81), with the variable r as the distance between the current evaluated surface point and an interior surface point in $-\Omega$. This constraint equation is a method developed by Bai to avoid singularities in eq. (77). According to Bai, the choice for interior points are arbitrary, they do not have to be physically

68 Richard L. Burden and J. Douglas Faires, *Numerical Analysis Ninth Edition,* (Boston: Brooks/Cole Cengage Learning, 2011), 243.

accessible in field measurement, and there must be the same number of interior points as the number of nodes on the source surface. Bai states, "Interior points are usually located on a surface that almost conforms to the source surface."[69]

Solving eq.(98) for Q_S gives

$$Q_S = [S^{S,interior}]^{-1} D^{S,interior} P_S \quad (99).$$

Substituting Q_S into eq.(81) gives

$$U^{ext} = [D^{S,ext} - S^{S,ext} * [S^{S,interior}]^{-1} * D^{S,interior}] * P_S \quad (100).$$

If $C = [D^{S,ext} - S^{S,ext} * [S^{S,interior}]^{-1} * D^{S,interior}]$, then the surface pressures are

$$P_s = C^{-1} U^{ext} \quad (101).$$

Once P_s is found, any far-field surfaces can be calculated using the equation

$$U^{ext} = C P_s \quad (102).$$

A c++ program is then written to perform eq.(100).

2.5 Implementation of NAH to my Research

As mentioned earlier, guitarists usually play chords, which are three or more harmonically-related notes that sound at the same time. Because solving the Helmholtz equation and studying the modes of the guitar is monochromatic, no studies exist on the analysis of the vibrating surface of a guitar when a chord is played. The superposition of waves principle states that any complex waveform (waves with multiple frequencies) is the summation of the individual frequency waves.[70] Because acoustic pressures are waves, the superposition principle can be applied to study a chord by summing the three frequency waves of a chord. I chose to investigate how an E chord vibrates by using NAH for each of the three notes in an E chord, E, G#, and B. The three pressure waves are then added to create a

69 Bai, "Application of BEM-Based Acoustic Holography," 537.
70 Richard Wolfson, *Essential University Physics: Volume I* (San Francisco: Pearson Education, 2007), 230.

unique vibratory pattern. By studying the unique vibratory pattern, the current microphone patterns can be justified, or a new, more optimal microphone pattern can be created to fully optimize the sound. In addition, cost-effective approaches must be utilized if my research is to be used in a recording studio or a commercial setting. Therefore, I am going to perform NAH in my apartment room and use a *Radioshack s*ound pressure level meter to obtain pressure data on the hologram to see if I can achieve accurate results comparable to the research done in laboratories.

Chapter 3: Experimental Procedure

3.1 Assumptions

The guitar that is being measured is a Yamaha FG-430. The guitar's dimensions are 16 inches by 19.5625 inches, and is 4.5 inches thick (from back plate to top plate). The surface discretization triangle base lengths range from 0.5 inches to 1.3 inches wide, and the hologram surface is at a half-inch above the guitar surface. I chose these values because the maximum wavelength measured is $\lambda_{max} = 27.5406$ inches, and having the triangles be an inch wide means that the elements are $\sim \frac{1}{27}\lambda_{max}$. This within the quarter of the wavelength restriction proposed by G.T. Kim, and therefore the program should be very accurate. The hologram pressure measurements were performed in my apartment, therefore some uncertainties in the data acquirement caused by room reflections and standing waves may be present. To avoid these reflections as much as possible, absorptive materials, such as carpets and blankets, were put on the floors and walls to absorb sound. Because a sound pressure level meter was used, only the magnitude of the pressure can be inputted into the program. Therefore, I want to see if accurate data can be acquired without knowledge of the phase and in an untreated environment. I am also assuming that the optimal microphone placements are areas of high pressure magnitude, since these areas have the most effect on microphones.

3.2 Experimental Tools and Implementation

The experimental tools used were the Ebow and the sound pressure level meter. The Ebow is a electromagnetic device that vibrates a string at a constant rate. Its original purpose and function is to create a purely musical effect by simulating the sound of playing a guitar with a violin bow. However, it can be used to vibrate the guitar at a constant rate, providing stable measurements and satisfying the

time-periodic conditions of the Helmholtz equation. The guitar was able to freely vibrate by taking a guitar stand and suspending it between two microphone stands, which held it in place with rubber bands. The guitar was then placed on the guitar stand with the top plate facing the ceiling, allowing the guitar to freely vibrate. A guitar string was then tuned to the correct frequency and the Ebow was placed on the guitar string. The sound pressure level meter was then placed on a microphone stand, allowing for the pressure meter to be placed accurately over the nodes at the correct height above the surface. For each node, the pressure was recorded by writing down the decibels. This procedure was implemented for each frequency.

3.3 Program Algorithm

The program used to implement NAH was written in c++. I programmed it so that it can handle general domains, so that the program can be used in the future for any vibrating source. The program has four input files. The first is a file containing a vertical list of the x,y,z coordinates of the surface nodes, followed by a space, then the list of node indexes that form a triangle on the surface. The nodes were computed by uploading a picture of my guitar into the graphic program *xfig*, scaling the picture so that an inch in *xfig* matches an inch of the guitar surface, and by drawing points approximately an inch apart. The triangles were then drawn by connecting the points, and the coordinates and triangle indexes were typed into the file. The second file is a vertical list of the measured pressures in decibels. It is important that the pressures are listed in the same order as the surface nodes in the first file. The program converts the decibels to pascals using eq.(1). The third file is a vertical list of the x,y,z coordinates of the interior surface. The interior surface was created by taking the guitar surface nodes and translating it into the interior by adding or subtracting 0.25 inches from either the x,y, or z surface coordinate. The fourth input file is a vertical list of the coordinates of the hologram surface. This is created in the same fashion as the interior surface, except the surface nodes are translated by 0.5 inches.

Firstly, the program reads in the first file and stores the data in an array of a struct named "triangles." This struct contains the x,y,z coordinates of each of the triangle's three vertices, plus the index number for each vertex. Then, the area of each triangle is calculated, which is used to calculate the Jacobian. This is done by treating the triangle as a composition of two vectors; if the triangle has vertices A, B, and C, then the two vectors are AB and AC. The area of the triangle is then found by taking the cross product of the two vectors, taking the magnitude of the resulting vector, and dividing the magnitude by 2.[71]

Next, the $D^{S,ext}$ matrix in eq.(100) is calculated. The program reads in the first holographic point coordinate from file four. Then the program focuses on the first surface node from file one. The program scans through all the surface triangles until it gets to a triangle that has the current surface node. A basis function is then defined for the triangle by using eq.(86). Then the triangle is transformed to (x', y', z') by using eqns.(75-76). Gaussian Quadrature, eqns.(93-97), is performed on the integrals, where the variable r is the distance from the evaluated gaussian point and the hologram point. The program then stores the integral answer in the correct row and column in the $D^{S,ext}$ matrix. This process is repeated until all integrals with the triangles containing the current surface node are evaluated. The next surface node in file one is then focused on, and the program sweeps for any triangle that contains the surface node, translates that triangle, and performs Gaussian Quadrature. Once the last surface node is reached in file one, the program moves to the next holographic point in file four, and the program starts over with the first surface node in file one. This process continues until the last holographic point in file four is reached. The same process is done for the $S^{S,ext}$ matrix.

For the $D^{S,interior}$ and $S^{S,interior}$ matrices in eq.(100), the same algorithm in finding the matrices $D^{S,ext}$ and $S^{S,ext}$ is used, except the holographic surface is replaced with the interior

71 John Taylor, "Area of a Triangle via the Cross product," http://www.jtaylor1142001.net/calcjat/Solutions/VCrossProduct/Cross-Product/Area-Triangle/CPAreaTri/CPAreaTri_Layers.htm (accessed March 5, 2012).

surface, file three. Once all the matrices are filled, the C matrix in eq.(101) is found by matrix multiplication and subtraction subroutines. The U^{ext} matrix is then filled with the converted pascal measurements from file two. The matrix C^{-1} is then found by using the LU factorization function in the c++ library TNT.[72] The surface pressures, in the order of the evaluated nodes, are then listed as the program output. Once all the frequency pressures are calculated, the magnitudes are summed to derive the pressure magnitudes for an E chord.

A vibrating sphere was used to test the program. A uniformly vibrating sphere (which only relies on the distance r) is governed by the equation

$$P(r)=(\frac{a}{r})\rho c\, U_a(\frac{ika}{ika-1})\exp[ik(r-a)] \quad (103)$$

where a is the sphere radius, ρ is the air density, c is the speed of sound in air, U_a is the vibrational velocity of the sphere surface, and k is the wavenumber.[73] If P_0 is the source pressure, then solving eq.(103) with r=a gives,

$$P_0=\rho c\, U_a(\frac{ika}{ika-1}) \quad (104).$$

Therefore,

$$P(r)=P_0(\frac{a}{r})\exp[ik(r-a)] \quad (105).$$

First, the construction of the surface pressures from the hologram using eq.(101) was tested. The parameters for this test are $P_0=1.0$ pascal, $a=0.1$ inches, a hologram surface 0.1 inches above the sphere ($r=0.2$ inches), and $k=0.046193$ (100Hz when c=13601.784 inches per second, which is the speed of sound in air at a temperature of 75 degrees Fahrenheit).[74] The interior surface was

72 Roldan Pozo, "Template Numerical Toolkit, An Interface for Scientific Computing in C++," Mathematical and Computational Sciences Division National Institute of Standards and Technology, http://math.nist.gov/tnt/ (accessed August 1, 2011).

73 Bai, "Application of BEM-Based Acoustic Holography," 538.

74 Eberhard Sengpiel, "Calculation of the Speed of Sound c in Air and the Effective Temperature," sengpielaudio http://www.sengpielaudio.com/calculator-speedsound.htm (accessed December 1, 2011).

a conformal sphere with a=0.09 inches. Solving eq.(105) with the above parameters, the pressure at the hologram is ~0.5 pascals. 0.5 pascals was then inputted into the U^{ext} matrix in eq.(100) and solved for P_s, expecting values around P_0. The sphere was discretized into 338 triangles, with 171 surface nodes. The sphere discretization was obtained online.[75] The calculated pressures at the surface nodes are represented in fig.2. Most of the pressures lie within ± 0.1 pascals of the correct value, 1.0 pascal, and the average error was 5.75%. However, some points had a significant amount of error. The minimum calculated pressure value was 0.637 pascals, the maximum calculated pressure value was 1.266 pascals, and the maximum pressure error for a point was 36.25%.

The NAH program was tested for different values of k that represented the entire fundamental frequency spectrum of the guitar. The program results for different k's are represented in figs.3 and 4. As figs.3 and 4 show, the NAH algorithm is very stable between 100-1,000Hz. This is easily shown in the average errors for each test. For 400Hz, the average error was 5.76%, with the minimum calculated pressure value being 0.637 pascals, the maximum calculated pressure value being 1.267pascals, and the maximum error for a point being 36.26%. For 1,000Hz, the average error was 5.81%, with the minimum calculated pressure value being 0.636 pascals, the maximum calculated pressure value being 1.271 pascals, and the maximum pressure error for a point being 36.36%. Notice the average error increases as k increases, but not by a significant amount, meaning that the program is stable in determining source pressures for 100-1,000Hz within an average error of less than 6%. Fig.6 shows the same results as fig.3, except using the visualization software *Medit,* which will be used to observe the pressure spots on the guitar. Unfortunately, I was not able to obtain a discretization of a sphere with more triangles to see if the error is significantly reduced. In addition, the distance between the hologram and the source surface contributes to the accuracy of the data. It is a general rule of thumb to

75 National Science Foundation, "A Finite Volume PDE Solver using Python," National Science Foundation, http://matforge.org/fipy/wiki/SurfaceOfSphere (accessed January 15, 2012).

have the hologram as close to the source surface as possible.[76]

Forward propagation, eq.(102), was then tested. Using $P_0 = 1.0$ pascal, the pressures were found at $r = 1.0$ (a surface 0.9 inches from the sphere). Using eq.(105), the expected pressure at $r = 1$ is $p(1) = 0.098621$ pascals. Fig.5 shows the program performance of forward propagation. The program is more accurate at calculating forward propagations, with the average error being 1.43%. The maximum calculated pressure value is 0.098621 pascals, the minimum calculated pressure value is 0.0972032 pascals, and the maximum pressure error for a point is 1.44%.

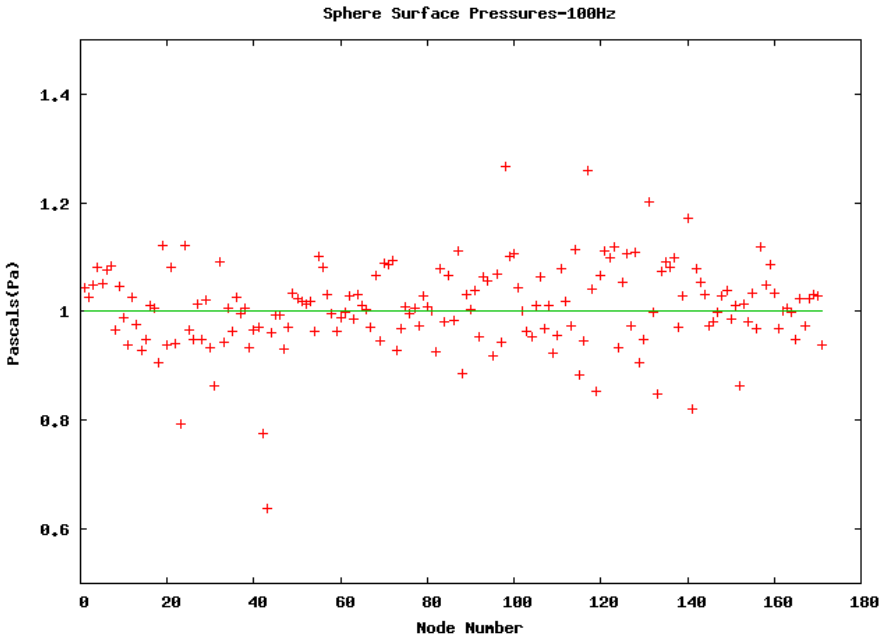

fig.2

76 Maynard, "Nearfield Acoustic Holography: I. Theory of Generalized Holography and the Development of NAH," 1405.

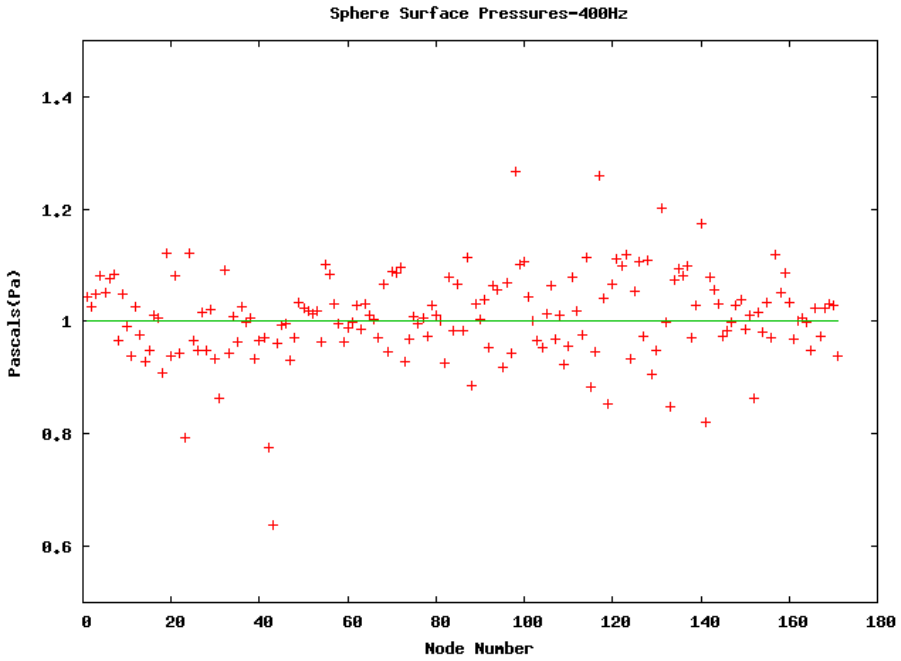
Sphere Surface Pressures-400Hz
Pascals(Pa)
Node Number
1.4
1.2
1
0.8
0.6
0
20
40
60
80
100
120
140
160
180

fig.3

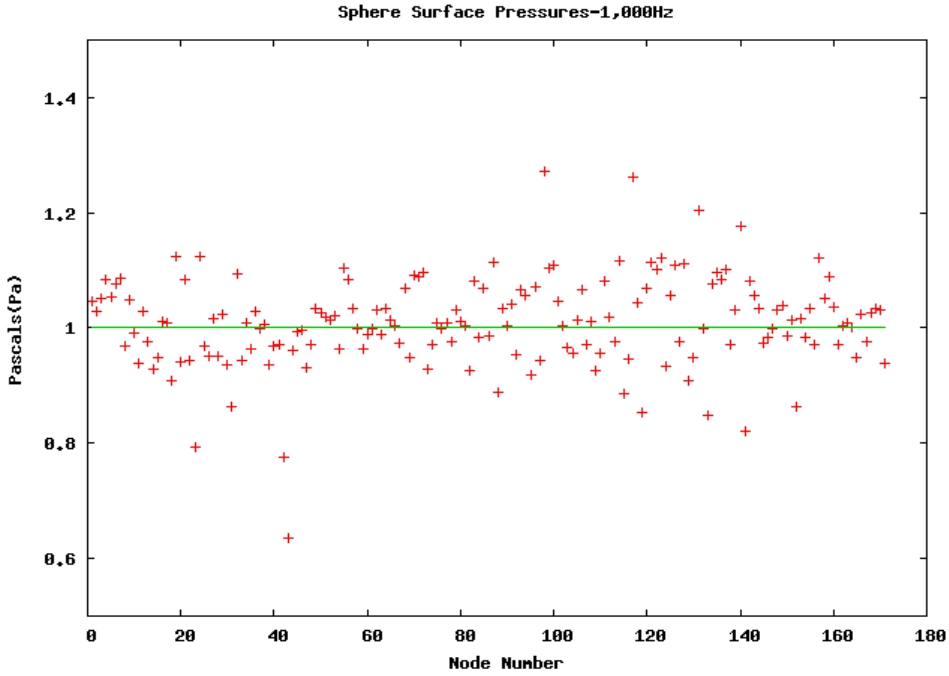
Sphere Surface Pressures-1,000Hz
Pascals(Pa)
Node Number
1.4
1.2
1
0.8
0.6
0
20
40
60
80
100
120
140
160
180

fig.4

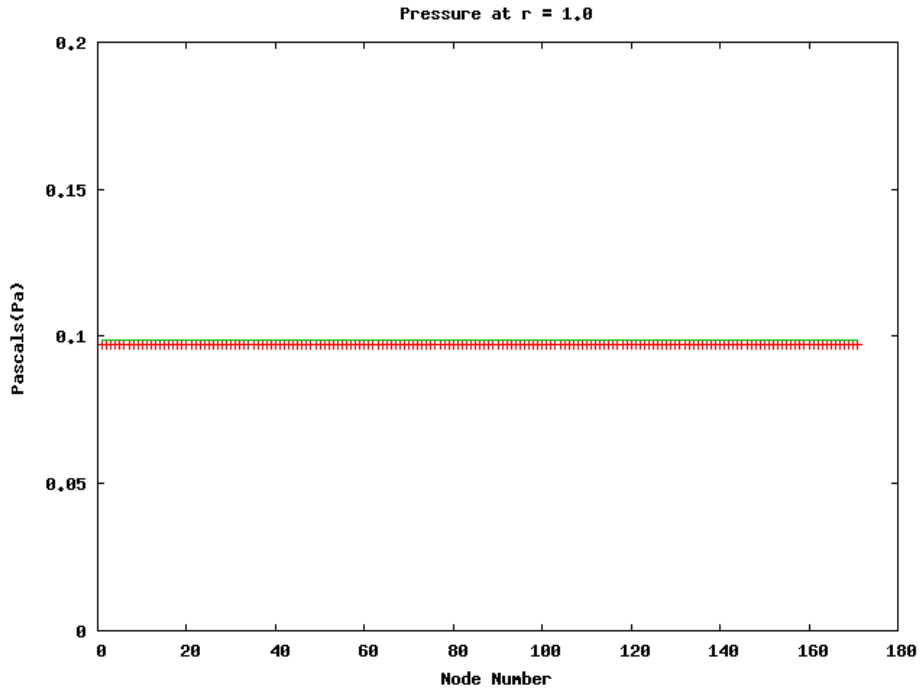
Pressure at r = 1.0
0.2
0.15
0.1
0.05
0
Pascals(Pa)
0
20
40
60
80
100
120
140
160
180
Node Number

fig.5

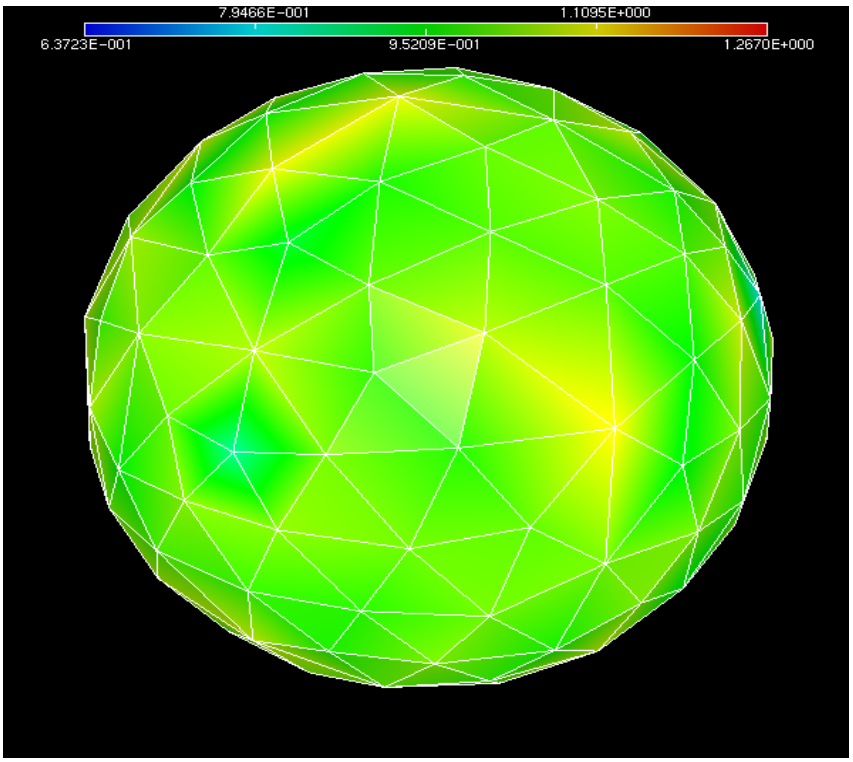
7.9466E-001
1.1095E+000
6.3723E-001
9.5209E-001
1.2670E+000

fig.6

Chapter 4

4.1 Results

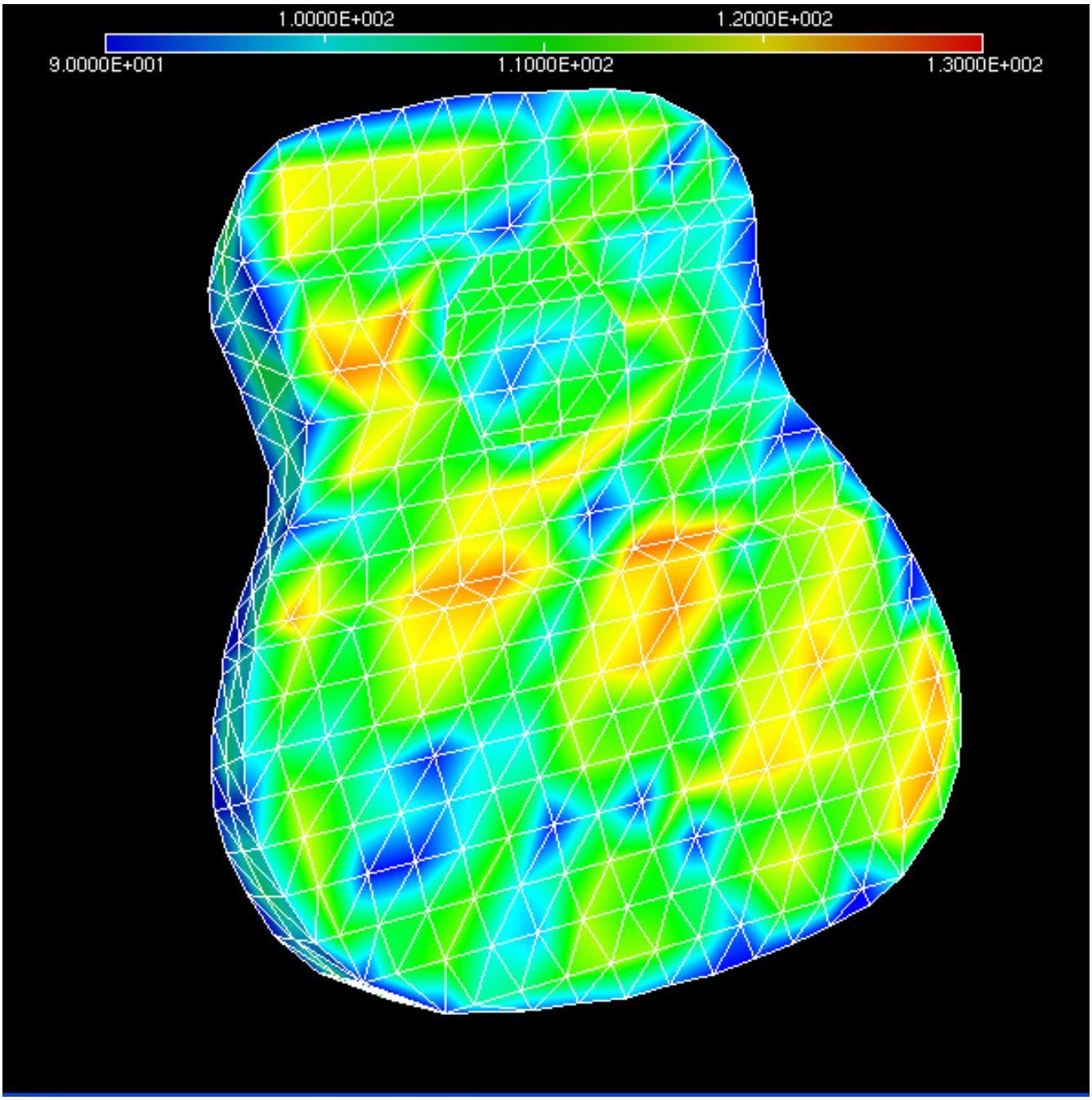

fig.7 Acoustic Pressure magnitudes of a E_4 note (329.63 Hz)

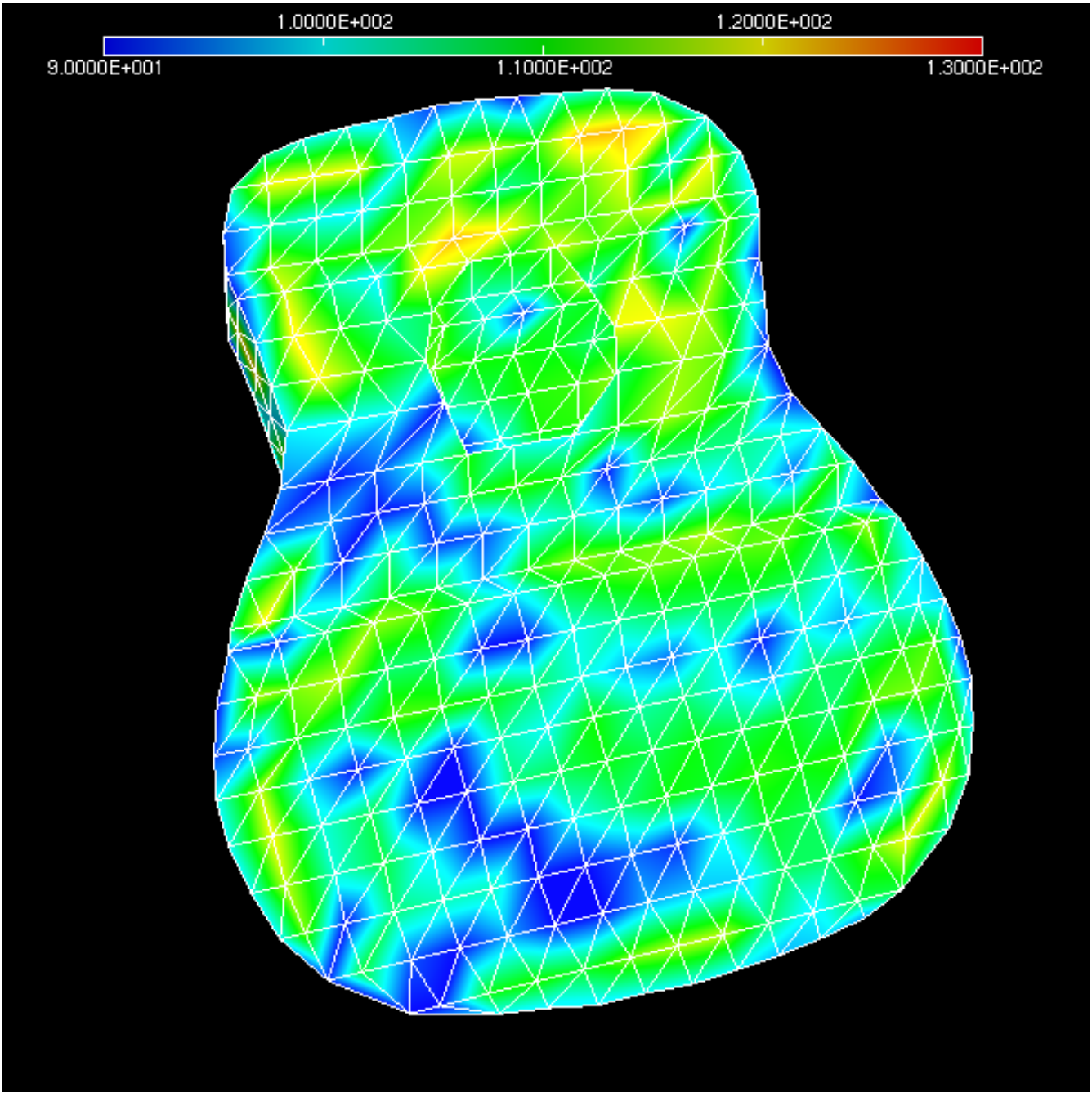

fig.8 Acoustic pressure magnitudes of a G#_4 note (415.30 Hz)

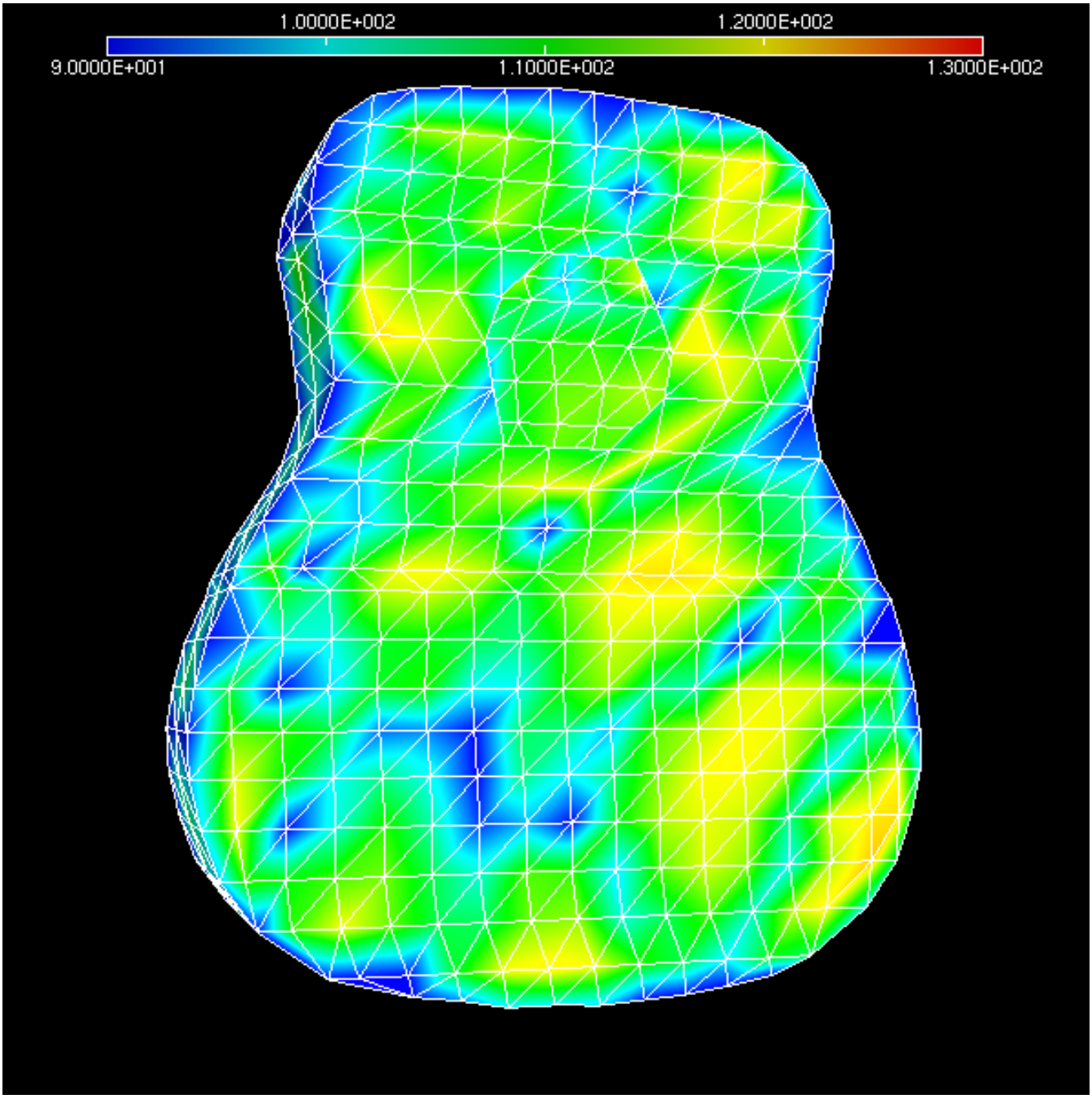

fig.9 Acoustic pressure magnitudes of a B_4 note (493.88 Hz)

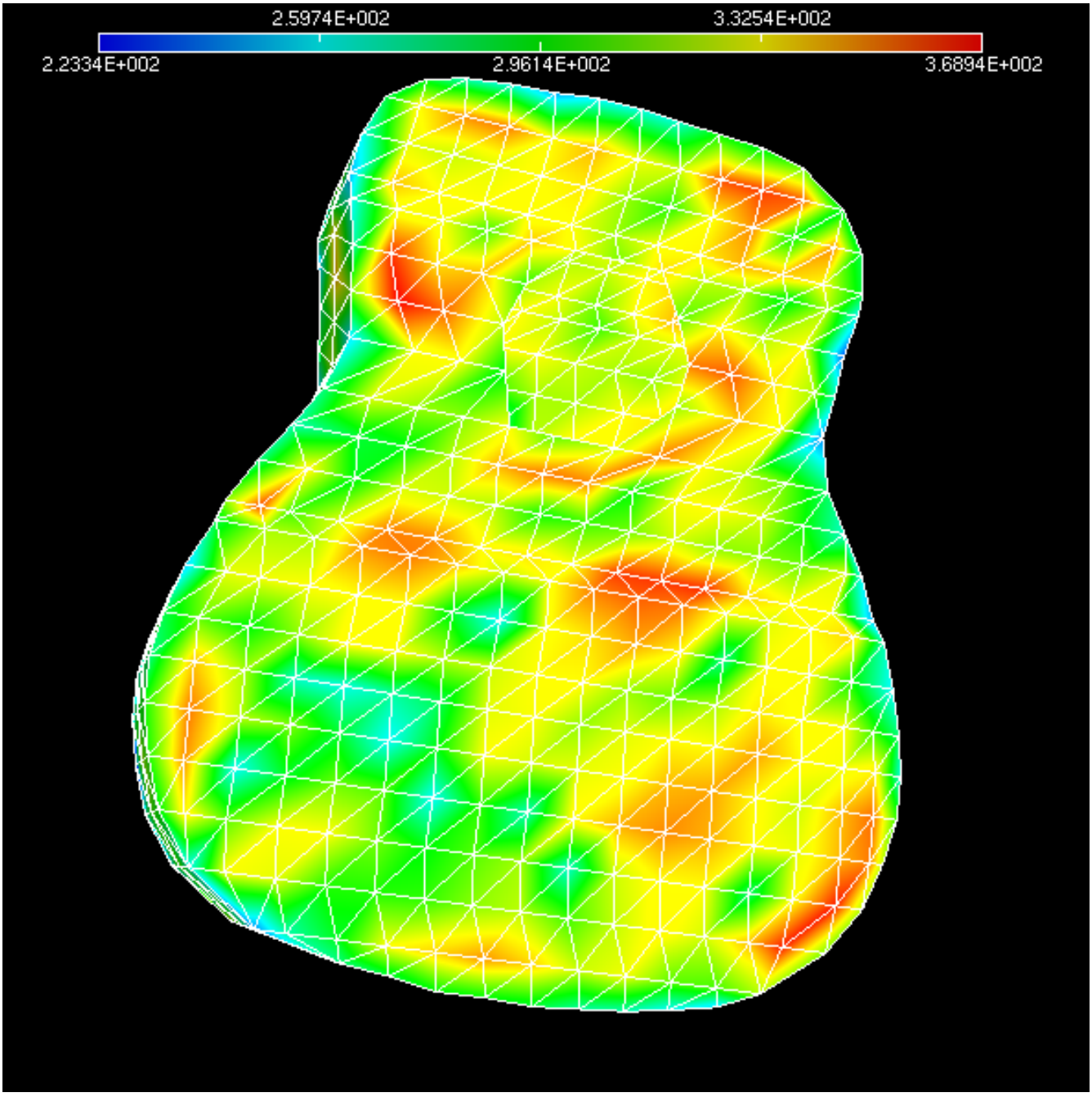

fig.10 Acoustic pressure magnitudes of an E chord

Forward Propagation from the guitar surface results at one foot above the guitar for E_4 (z=16.5)

x	y	Calculated (dB)	Real (dB)	Error (%)
7.94	6.31	82	84	2.38
8.56	15.62	83	82	1.21
2.56	2.35	83	79	5.06

fig.11

Forward propagation from the guitar surface results at one foot above the guitar for G#_4 (z=16.5)

x	y	Calculated (dB)	Real (dB)	Error (%)
7.94	6.31	93	74	25.67
8.56	15.62	91	70	30
2.56	2.35	92	66	39.4

fig.12

Forward propagation from the guitar surface results at one foot above the guitar for B_4 (z=16.5)

x	y	Calculated (dB)	Real (dB)	Error (%)
7.94	6.31	84	73	15.06
8.56	15.62	81	60	35
2.56	2.35	78	57	36.84

Fig.13

4.2 Interpretation of Results

After running the NAH algorithm to determine the source pressures, eq.(101), I used the "feeling test" to verify the results of the program. By placing one's hand on the guitar surface, one can feel the areas of most and least vibration. While this test gives no accuracy to the actual pressure values, it gives an indication on whether the program was able to find the correct spots of most and least vibration. Performing the "feeling test" showed good agreement with what the program calculated (figs. 7-10).

I then ran the program for an isosurface located one foot above the guitar to study the far-field. The isosurface was a rectangle with coordinates $-2.3125 \le x \le 20.5$, $-2.3125 \le y \le 23.5625$, $z = 16.5$ (z at the top plate is $z = 4.5$). The isosurface had the same number of nodes as the guitar surface, so eq.(102) could be used. The isosurface was then calculated based on the surface pressures. However, the program did not agree with experimental measures one foot above the guitar. I carried this out by selecting three isosurface points and finding the pressure data using the sound pressure level meter. I first carried out this test with the E note. This is shown in fig.11. The maximum error for an evaluated isosurface point is 5.06%, which is an acceptable amount of error. However, when repeated for the G# and B note, the points measured on the isosurface did not agree with the program results, which is shown in figs.12-13. Most of the errors on the evaluated isosurface points were between 30-40%. This is a significant and unacceptable amount of error. Therefore, the program failed to calculate accurate pressures in the far-field.

As the test problems on the sphere show, the program should be very accurate in calculating far-field pressures (below 2% error). Therefore, the significant errors in calculating the far-field are a result of the measuring process. I postulate that the two factors I did not take into account, the room acoustics and the phase, contributed to inaccurate far-field predictions.

Firstly, the guitar measurements were not taken in an acoustically treated room. The room has

hard, parallel walls with some absorptive material, but not acoustically treated absorptive material that absorbs all frequencies, so therefore the room is prone to standing and reflecting waves. These second-order waves can have a drastic effect on the initial sound wave coming from the guitar. Since these waves are at the same frequency as the incident waves, and they are delayed from the incident wave by the time is takes to reflect off a wall, the reflective waves can either boost the incident wave at one point (constructive interference) or reduce the incident wave or even cancel portions of it out (destructive interference). These reflections and standing waves can alter sound waves by as much as 20dB or more.[77] Since solving the Helmholtz equation only takes into account incident waves, these reflective waves can alter both the initial hologram measurements and the isosurface measurements.

In addition, phase relations were not taken into account, since a sound pressure level meter does not consider phase. For example, parts of the measured hologram could have been in the compression part of a wave (positive pascals), or in a refractive part of a wave (negative pascals) at a particular time. Usually, NAH is performed with both pressure-sensitive and phase-sensitive microphones. These microphones are used with Lock-in amplifiers, which measure the pressure and the phase by comparing the wave to a sine wave vibrating at the same frequency as the source. Therefore, my goal of seeing if accurate results could still be obtained using a sound pressure level meter in my apartment mostly failed.

There may also be additional factors that contributed to the measurement error. Firstly, my accuracy of placing the sound pressure level meter at the exact hologram coordinate above the guitar may have been off. I marked the nodal areas on my guitar, and used it as a sight to aim the sound level meter. Therefore, it is very possible that I would have been off in some of my measurements by around half of the element size. Because more nodal activities occur on the surface of a guitar at higher frequencies, the inaccuracy of the measurement locations can significantly contribute to the error and

77 Huber, *Modern Recording Techniques,* 98-99.

be a probable cause on why the errors were significant for the higher frequencies. In addition, guitar strings contain many overtones. While I did my best to subdue the overtones and make the fundamental frequency the most prominent, the overtones are still present and contribute to the vibratory pattern of the guitar. Since the main assumption of solving the Helmholtz equation is that the source is only vibrating at one frequency, the fact that the present overtones were not taken into account can contribute to the error.

However, the program was good at determining surface vibration spots. I hypothesize that this worked because since the hologram was recorded at such close distances to the surface, the surface node right below it has the most influence on the hologram pressure level. This is in direct contrast to the far-field, where many points on the surface affect the pressure level on one point of the isosurface. Because the hologram was recorded at a very close distance, the signal to noise ratio on the sound level meter was very high at points of high vibrations, so room reflections have a significantly less effect on the measured data (since the incident signal is significantly louder than the reflective signal). This, however, cannot be said around areas that have lower pressure values, since the reflective waves are not as masked by the incident waves, as in the high pressure case. Therefore, the points of relatively low pressure can be distorted by the room acoustics.

Since only the positive pascal values were inputted into the program, no inferences on phase can be made at the source surface. In addition, since the program failed to predict the far-field, the actual pressure values on the source surface may not be correct. While obtaining correct pressure values is very important in the mathematical sense, the guitar is an extremely dynamic instrument, meaning it does not vibrate at a constant pressure level as does an engine, or a loudspeaker set to output at a specific volume. A guitarist is constantly changing dynamics by playing both loud and soft in different musical passages. Therefore the actual pressure values are not very important since they are constantly changing when a performer plays. Finding the areas of vibration are more important for

recording purposes than knowing the pressure values, and the program did succeed in finding these spots. However, precise pressure values may be important for a guitar luthier, since the luthier may want the guitar to vibrate at a specific decibel level to ensure that the guitar is loud enough to project to the audience.

Unfortunately, a major aspect of NAH, the ability to study the far-field by only knowing the surface pressures, was not able to be utilized. Therefore, far-field predictions cannot be made with a sound pressure level meter in an untreated room. However, recording studios could still implement these techniques because studios are acoustically treated and have accurate microphones that are also sensitive to phase. Using current recording software, such as *Pro Tools* or *Logic*, studios can accurately analyze a waveform's magnitude and phase, and be able to carry out the NAH algorithm successfully.

4.3 Optimal Microphone Placements

Since the program predicted the surface vibration spots accurately, close microphone placements can be determined. The first important general conclusion made is that high vibrational areas on the guitar change per frequency, as we saw for the violin. Therefore, microphones need to be placed according to what frequencies the guitarist is playing. If the guitarist is utilizing the entire frequency spectrum, then a compromise may have to be made on where to place the microphones.

Observing fig.7, a E_4 note mostly vibrates in two places, around the sound-hole and on the lower-right of the guitar (all references to guitar locations will be made based on the perspective of the figure). Observing fig.8, a G#_4 vibrates more on the top part of the guitar than on the bottom part, unlike the E_4 note. Observing fig.9, a B_4 note vibrates more at the left part of the sound-hole and around the pick guard, and on the lower-right part of the guitar. It is interesting to note that the bottom-left does not vibrate significantly for all three of the frequencies.

Fig.10 shows the vibrational magnitudes of an E chord, which was created by summing the

three frequency magnitudes. Observing fig.10, the area of most vibration is around the sound-hole, in particular the left side (which was significantly confirmed by the “feeling test”). The next area of vibration is the lower-right part of the guitar. Using these results, a new, optimal microphone placement would then be to place a microphone aiming at the left part of the sound hole, and at the lower right part of the body. Because the bottom-left of the guitar does not significantly vibrate, a microphone should not be placed around that spot.

4.4 Future Research

As previously discussed, obtaining more accurate data will fully utilize the power of NAH, and far-field predictions can be made. However, NAH can be used to extensively study parts of the guitar that I was not able to cover. First of all, I have shown that guitar surface vibrational patterns change depending on the frequency. Therefore, if one had the proper equipment to implement NAH quickly and effectively, one could observe how a guitar vibrates for each note in the entire guitar spectrum (E_2 to D_6). Then, one can simply add any combination of notes to see the vibrational patterns for a multitude of chords. Implementing this would be more realistic in recording situations because a guitarist usually utilizes all six strings when playing a chord by playing the three fundamental chord notes in different octaves. In addition, one could analyze more complex chords, such as seventh and ninth chords. Also, because NAH was used, the notes and chords can also be analyzed in the far-field. Because using a sound pressure level meter in an untreated environment did not fully work, research done with other cost-effective measuring devices and technology can be conducted to see if more accurate results can be obtained. Another area where NAH can be used is in guitar construction. By analyzing a sonically decent guitar, one can then build a guitar by mimicking the vibrational patterns.

Works Cited

Bai, Mingsian R. “Application of BEM (Boundary Element Method)-Based Acoustic Holography to Radiation Analysis of Sound Sources with Arbitrarily Shaped Geometries.” *Journal of the Acoustical Society of America* 92, no. 1 (1992): 533-549.

Barnett, Alex, and Leslie Greengard. “A New Integral Representation for Quasi-Periodic Scattering Problems in Two Dimensions.” *BIT Numerical Mathematics* 51 (2011): 67-90.

Burden, Richard L., and J. Douglas Faires. *Numerical Analysis Ninth Edition.* Boston: Brooks/Cole Cengage Learning, 2011.

Cuzzucoli, Giuseppe, and Vincenzo Lombardo. “A Physical Model of the Classical Guitar, Including the Player's Touch.” *Computer Music Journal* 83, no. 2 (1999): 52-69.

Derveaux, Gregoire, Eliane Becache, Antoine Chaigne, and Patrick Joly. “Numerical Simulation of a Guitar.” *Computers and Structures* 83 (2005): 107-126.

French, Richard Mark. *Engineering the Guitar: Theory and Practice.* New York: Springer Science, 2009.

Ganesh, Mahadevan, and S.C. Hawkins. “A Fully Discrete Galerkin Method for High Frequency Exterior Acoustic Scattering in Three Dimensions,” *Journal of Computational Physics* 230 (2011): 104-125.

Huber, David Miles and Robert E. Runstein. *Modern Recording Techniques 7th Edition.* Oxford: Focal Press, 2010.

Hunter, Peter. “FEM/BEM Notes.” New Zealand: The University of Auckland, Department of Engineering Science, 1997.

Kim, G.T., and B.H. Lee. “3-D Sound Source Reconstruction and Field Prediction Using the Helmholtz Integral Equation.” *Journal of Sound and Vibration* 136, no. 2 (1990): 245-261.

Kinsler, Lawrence E., Austin R. Frey, Alan B. Coppens, and James V. Sanders. *Fundamentals of Acoustics, Third Edition.* New York: John Wiley & Sons, 1982.

Maynard, J.D., E.G. Williams, and Y. Lee. “Nearfield Acoustic Holography: I. Theory of Generalized Holography and the Development of NAH.” *Journal of the Acoustical Society of America* 78, no. 4 (1985): 1395-1413.

National Science Foundation. “A Finite Volume PDE Solver using Python.” National Science Foundation. http://matforge.org/fipy/wiki/SurfaceOfSphere (accessed January 15, 2012).

Pozo, Roldan. “Template Numerical Toolkit, An Interface for Scientific Computing in C++.” Mathematical and Computational Sciences Division National Institute of Standards and Technology. http://math.nist.gov/tnt/ (accessed August 1, 2011).

Russell, Daniel. “Acoustics and Vibrations of Guitars.” Penn State Acoustics. http://www.acs.psu.edu/drussell/guitars.html (accessed March 5, 2012).

Sengpiel, Eberhard. “Calculation of the Speed of Sound c in Air and the Effective Temperature.” sengpielaudio. http://www.sengpielaudio.com/calculator-speedsound.htm (accessed December 1, 2011).

Strauss, Walter A. *Partial Differential Equations: An Introduction, Second Edition.* New Jersey: John Wiley & Sons, 2008.

Taylor, John. “Area of a Triangle via the Cross product.” http://www.jtaylor1142001.net/calcjat/Solutions/VCrossProduct/Cross-Product/Area-Triangle/CPAreaTri/CPAreaTri_Layers.htm (accessed March 5, 2012).

Tronel, Gregoire. “Near-field Acoustic Holography: The Frame Drum.” Powerpoint Presentation, University of Illinois at Urbana-Champaign, 2010.

Wang, Lily M., and Courtney B. Burroughs. “Acoustic Radiation from Bowed Violins.” *Journal of the Acoustical Society of America* 110, no. 1 (2001): 543-555.

White, Paul. “Recording Acoustic Guitar,” *Sound on Sound,* August 2001. http://www.soundonsound.com/sos/aug01/articles/recacgtr0801.asp (accessed March 24, 2012).

Wolfson, Richard. *Essential University Physics: Volume I.* San Francisco: Pearson Education, 2007.

Wu, Sean F. “Hybrid Near-field Acoustic Holography.” *Journal of the Acoustical Society of America* 115, no. 1 (2004): 207-217.

Wu, Sean F. “Techniques for Implementing Near-Field Acoustical Holography.” *Sound and Vibration,* February 2010, 12-16.